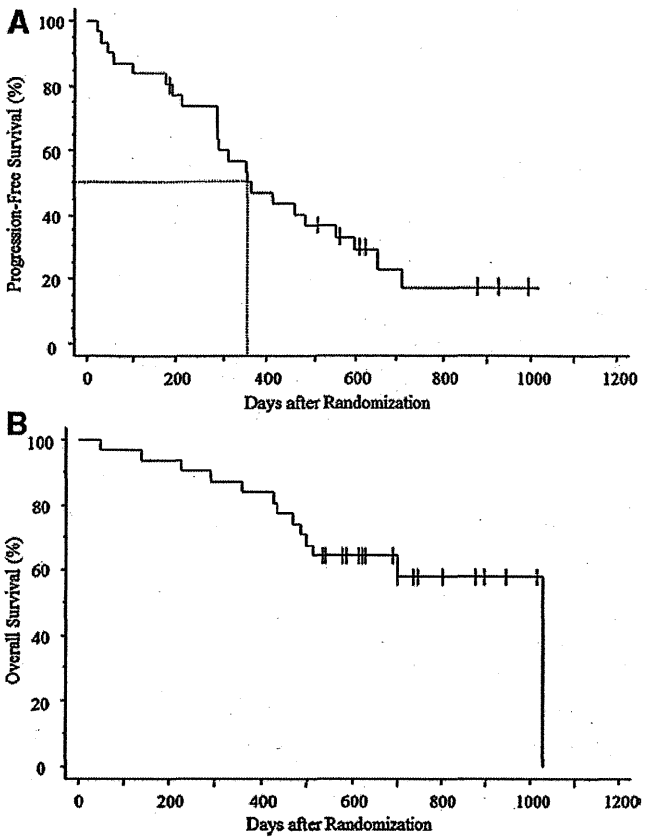

FIGURE 1. Progression-free survival and overall survival. Kaplan–Meier curves for progression-free survival are shown for the progression-free survival population (*A*), and Kaplan–Meier curves for overall survival are shown in (*B*). In (*A*) and (*B*), tick marks indicate patients for whom data were censored.

TABLE 3. Safety—Hematologic and Nonhematologic Toxicity

	NCI-CTC Grade					Grade
	1	2	3	4	5	3–4 (%)
Hematologic adverse events						
Leukocytopenia	2	1	0	0	0	0
Neutropenia	0	1	0	0	0	0
Anemia	6	4	0	0	0	0
Thrombocytopenia	2	1	0	0	0	0
AST/ALT	7	2	6	0	0	19
T-Bil	3	1	0	0	0	0
Creatinine	5	1	0	0	0	0
Hyperkalemia	7	0	0	0	0	0
Nonhematologic adverse events						
Pneumonitis	0	0	0	0	1[a]	3
Rash	12	10	1	0		3
Nail change	4	2	0	0		0
Stomatitis	3	0	0	0		0
Alopecia	3	0	0	0		0
Appetite loss	7	2	1	0		3
Nausea/vomiting	1	0	0	0		0
Diarrhea	9	2	1	0		3
Constipation	2	0	0	0		0
Fatigue	4	1	0	0		0

NCI-CTC, National Cancer Institute Common. Terminology Criteria; AST, androgen suppression therapy; ALT, alanine aminotransferase; T-Bil, total bilirubin.
[a]Treatmant-related death.

erlotinib. No patient was treated with platinum doublets. Six patients did not receive any second-line treatment.

DISCUSSION

This is the first study targeting elderly patients with EGFR-mutated NSCLC. In this study, gefitinib displayed remarkable efficacy without increased toxicity.

We have previously reported a single-arm phase II study in which gefitinib was administered to frail patients with poor PS or elderly patients who were unfit to undergo treatment with cytotoxic agents.[20] In that study, the patients enrolled were 20 to 74 years old with a PS of 3 to 4, 75 to 79 years old with a PS of 2 to 4, and aged 80 years or older (super-elderly) with a PS of 1 to 4. Patients older than 74 years of age accounted for 39% of the total enrolled patients but, nevertheless, OS was 17.8 months (Table 4). The current study strengthened the conclusion of the previous one and provided more information with respect to the efficacy of gefitinib in elderly NSCLC patients with EGFR mutation.

We defined elderly patients as those who were 75 years old and older. Many studies and subgroup analyses were performed by considering elderly cases as 70 years of age or older, especially in Western countries. We have regarded patients aged 70 to 75 years as being treatable with platinum-based chemotherapy. In fact, patients in this age group were enrolled in the NEJ002 study and were able to withstand treatment with platinum doublet. Accordingly, we excluded this group of patients from enrollment in the present study. Considering the aging of population structures and the increased longevity in Japan, we thought that the candidate selection for this study was reasonable.

Currently, in elderly patients, single-agent chemotherapy with a third generation agent (vinorelbine, gemcitabine, or taxanes) is the recommended approach according to the American Society of Clinical Oncology guidelines.[2–7] Gefitinib, which is considered minimally toxic, is often selected for the treatment of advanced NSCLC in elderly patients. Crino et al. performed a randomized phase II study (Gefitinib Versus Vinorelbine in Chemotherapy-Naïve Elderly Patients With Advanced Non-Small-Cell Lung Cancer [INVITE]) of gefitinib versus vinorelbine treatment in 196 chemotherapy-naive unselected elderly patients.[21] There were no statistical differences between gefitinib and vinorelbine in terms of PFS, OS, and ORR. Their study showed obviously lower efficacy of gefitinib in nonselected patients, as compared with the results shown from our study of EGFR-mutated patients.[22–24] These differences in effectiveness among studies highlight the importance of selection of patients by EGFR mutation analysis when administrating gefitinib. Furthermore, in another study of gefitinib treatment in Japanese patients aged

TABLE 4. Pivotal Clinical Trials of Cytotoxic Agents or EGFR-TKIs in Elder Patients With NSCLC and Recent Trials of Gefitinib in Patients selected by EGFR Mutation

Trial	Treatment	*n*	ORR (%)	PFS (mo)	MST (mo)	*p* Value
Cytotoxic agent in unselected elder patients						
ELVIS[3]	VNR	76	19.7		6.4	0.04
	BSC	78	—		4.8	
MILES[5]	VNR + GEM	232	21	4.1	6.9	NS
	GEM	233	16	4.4	6.5	
	VNR	233	18	4.4	8.3	
WJTOG9904[7]	DTX	89	22.7	5.5	14.3	$p = 0.138$
	VNR	91	9.9	3.1	9.9	
EGFR-TKI in unselected elder patients						
Ebi N.[25]	Gefitinib	49	25	4	10	—
Crino L.[21]	Gefitinib	97	3.1	2.7	5.9	NS
	VNR	99	5.1	2.9	8.0	
Jackman D. M.[27]	Erlotinib	80	10	3.5	10.9	—
Chen Y. M.[28]	Erlotinib	57	22.8	4.6	11.7	$p = 0.70$
	VNR	56	8.9	2.5	9.3	
EGFR-TKI in selected younger patients						
WJTOG3405[14]	Gefitinib	86	62.1	9.2	Immature	$p < 0.001$ (PFS)
	CDDP + DTX	86	32.2	6.3		
NEJ002[15]	Gefitinib	114	73.7	10.8	30.5	$p < 0.001$ (PFS)
	CBDCA + PTX	110	30.7	5.4	23.6	
EGFR-TKI in selected elder patients (current study)						
NEJ003	Gefitinib	31	74.2	12.1	33.8	—

ELVIS, Elderly Lung Cancer Vinorelbine Italian Study; MILES, Multicenter Italian Lung Cancer in the Elderly Study; ORR, overall response rate; PFS, progression-free survival; MST, median survival time; VNR, vinorelbine; BSC, best supportive care; NS, not significant; GEM, gemcitabine; DTX, docetaxel; EGFR-TKI, epidermal growth factor receptor–tyrosine kinase inhibitors; CDDP, cisplatin; CBDCA, carboplatin; PTX, paclitaxel.

75 or older, which included about 40% of the patients who were examined for EGFR mutations and 14% of the patients with EGFR-mutated tumors, the response rate was only 25%.[25] Meanwhile, there have been a few studies of treatment for elderly unselected patients with erlotinib, which is supposed to be more toxic than gefitinib as the administered dose was set near the maximum tolerance dose.[26,27] The response rates in these studies were 10% or less, which were similar to those from the gefitinib studies conducted in Western populations (Table 4). In the other Asian study, erlotinib was compared with vinorelbine treatment in patients aged 70 or older.[28] That study demonstrated that erlotinib yielded a higher response rate and PFS than vinorelbine. The percentage of mutation-positive patients was 30% of those who were examined for EGFR mutations in the erlotinib group. This high proportion might have contributed to the better results of the erlotinib group. The treatment of unselected NSCLC patients with erlotinib was also as ineffective as with gefitinib. Efficacy results in patients selected by EGFR mutation in the current study were substantially superior to those observed in the studies of gefitinib or erlotinib with unselected cases. Surprisingly, the median PFS and 2 year-survival rate here were comparable with results obtained in NEJ002 (12.3 versus 10.8 months, 58% versus 61%, respectively) despite the limited enrollment of an elderly population in this study. These two studies, namely NEJ002 and NEJ003, have very similar backgrounds as they were performed during almost the same time period at identical institutions. It was suggested that gefitinib displayed similar efficacy in elderly patients when compared with their younger counterparts (Table 4). Although the current phase II study could not verify whether gefitinib prolonged PFS in elderly patients in comparison with younger patients, gefitinib might still prove to be the most suitable agent for elderly patients with EGFR-mutated NSCLC.

Elderly patients generally have more comorbidities and lower organ function than younger patients. Treatment-related toxicity in the elderly is a more significant issue than for younger patients. A subgroup analysis of BR.21 showed that elderly patients treated with erlotinib displayed similar efficacy with respect to survival and quality of life as their younger counterparts but experienced greater toxicity.[27] In the current study, toxicity was generally mild and predictable. Rash, diarrhea, and elevation of transaminase were observed frequently, similar to other studies with EGFR-TKIs. The single case of treatment-related death that occurred in our study was because of ILD, although this condition was not found in other patients. The frequency of ILD in the current study was comparable with that previously reported in Japan. Unfortunately, this patient did not respond to treatment with a large dose of corticosteroid, which is generally used for such conditions.[17,29] Advanced age and smoking, preexisting ILD, and poor performance status have been reported as risk factors for ILD during treatment with gefitinib.[17] Elderly patients treated with EGFR-TKIs should be monitored with further caution for ILD. On the whole, gefitinib was found to be a well-tolerated therapy for elderly patients with mutated NSCLC.

In conclusion, first-line gefitinib treatment is highly effective with acceptable toxicity for elderly patients with advanced NSCLC harboring EGFR mutations. Together with our previous studies (NEJ001, NEJ002), gefitinib is shown to be an ideal therapy for all types of NSCLC patients with EGFR mutation.

ACKNOWLEDGMENT

This work was supported by a grant from the Tokyo Cooperative Oncology Group.

REFERENCES

1. Center for Cancer Control and Information Services, National Cancer Center, Japan. Web site. Available at: http://ganjoho.jp/professional/statistics /statistics.html/. Accessed February 1, 2011.
2. Azzoli CG, Baker S Jr, Temin S, et al. American Society of Clinical Oncology. American Society of Clinical Oncology Clinical Practice Guideline update on chemotherapy for stage IV non-small-cell lung cancer. *J Clin Oncol* 2009;27:6251–6266.
3. Effects of vinorelbine on quality of life and survival of elderly patients with advanced non-small-cell lung cancer. The Elderly Lung Cancer Vinorelbine Italian Study Group. *J Natl Cancer Inst* 1999;91:66–72.
4. Frasci G, Lorusso V, Panza N, et al. Gemcitabine plus vinorelbine versus vinorelbine alone in elderly patients with advanced non-small-cell lung cancer. *J Clin Oncol* 2000;18:2529–2536.

5. Gridelli C, Perrone F, Gallo C, et al. MILES Investigators. Chemotherapy for elderly patients with advanced non-small-cell lung cancer: the Multicenter Italian Lung Cancer in the Elderly Study (MILES) phase III randomized trial. *J Natl Cancer Inst* 2003;95:362–372.
6. Gridelli C, Aapro M, Ardizzoni A, et al. Treatment of advanced non-small-cell lung cancer in the elderly: results of an international expert panel. *J Clin Oncol* 2005;23:3125–3137.
7. Kudoh S, Takeda K, Nakagawa K, et al. Phase III study of docetaxel compared with vinorelbine in elderly patients with advanced non-small-cell lung cancer: results of the West Japan Thoracic Oncology Group Trial (WJTOG 9904). *J Clin Oncol* 2006;24:3657–3663.
8. E. A. Quoix, J. Oster, V. Westeel, E. Pichon, G. Zalcman, L. Baudrin, A. Lavole, J. Dauba, M. Lebitasy, and B. J. Milleron,. Weekly paclitaxel combined with monthly carboplatin versus single-agent therapy in patients age 70 to 89: IFCT-0501 randomized phase III study in advanced non-small cell lung cancer (NSCLC). *J Clin Oncol* 28:18s, 2010 (suppl; abstr 2)
9. Lynch TJ, Bell DW, Sordella R, et al. Activating mutations in the epidermal growth factor receptor underlying responsiveness of non-small-cell lung cancer to gefitinib. *N Engl J Med* 2004;350:2129–2139.
10. Paez JG, Jänne PA, Lee JC, et al. EGFR mutations in lung cancer: correlation with clinical response to gefitinib therapy. *Science* 2004;304:1497–1500.
11. Kris MG, Natale RB, Herbst RS, et al. Efficacy of gefitinib, an inhibitor of the epidermal growth factor receptor tyrosine kinase, in symptomatic patients with non-small cell lung cancer: a randomized trial. *JAMA* 2003;290:2149–2158.
12. Fukuoka M, Yano S, Giaccone G, et al. Multi-institutional randomized phase II trial of gefitinib for previously treated patients with advanced non-small-cell lung cancer (The IDEAL 1 Trial) [corrected]. *J Clin Oncol* 2003;21:2237–2246.
13. Mok TS, Wu YL, Thongprasert S, et al. Gefitinib or carboplatin-paclitaxel in pulmonary adenocarcinoma. *N Engl J Med* 2009;361:947–957.
14. Mitsudomi T, Morita S, Yatabe Y, et al.; West Japan Oncology Group. Gefitinib versus cisplatin plus docetaxel in patients with non-small-cell lung cancer harbouring mutations of the epidermal growth factor receptor (WJTOG3405): an open label, randomised phase 3 trial. *Lancet Oncol* 2010;11:121–128.
15. Maemondo M, Inoue A, Kobayashi K, et al. North-East Japan Study Group. Gefitinib or chemotherapy for non-small-cell lung cancer with mutated EGFR. *N Engl J Med* 2010;362:2380–2388.
16. Yoshizawa H, Kobayashi K, Inoue A, Maemondo M, Sugawara S, Oizumi S, et al. QOL Analysis from NEJ 002 Study Comparing Gefitinib to Chemotherapy for Non-Small Cell Lung Cancer with Mutated EGFR. ESMO Annual meeting 2011 (abst.364 PD).
17. Kudoh S, Kato H, Nishiwaki Y, et al. Japan Thoracic Radiology Group. Interstitial lung disease in Japanese patients with lung cancer: a cohort and nested case-control study. *Am J Respir Crit Care Med* 2008;177:1348–1357.
18. Nagai Y, Miyazawa H, Huqun, et al. Genetic heterogeneity of the epidermal growth factor receptor in non-small cell lung cancer cell lines revealed by a rapid and sensitive detection system, the peptide nucleic acid-locked nucleic acid PCR clamp. *Cancer Res* 2005;65: 7276–7282.
19. Sakakibara T, Inoue A, Sugawara S, et al. Randomized phase II trial of weekly paclitaxel combined with carboplatin versus standard paclitaxel combined with carboplatin for elderly patients with advanced non-small-cell lung cancer. *Ann Oncol* 2010;21:795–799.
20. Inoue A, Kobayashi K, Usui K, et al. North East Japan Gefitinib Study Group. First-line gefitinib for patients with advanced non-small-cell lung cancer harboring epidermal growth factor receptor mutations without indication for chemotherapy. *J Clin Oncol* 2009;27:1394–1400.
21. Crinò L, Cappuzzo F, Zatloukal P, et al. Gefitinib versus vinorelbine in chemotherapy-naive elderly patients with advanced non-small-cell lung cancer (INVITE): a randomized, phase II study. *J Clin Oncol* 2008;26:4253–4260.
22. Inoue A, Suzuki T, Fukuhara T, et al. Prospective phase II study of gefitinib for chemotherapy-naive patients with advanced non-small-cell lung cancer with epidermal growth factor receptor gene mutations. *J Clin Oncol* 2006;24:3340–3346.
23. Asahina H, Yamazaki K, Kinoshita I, et al. A phase II trial of gefitinib as first-line therapy for advanced non-small cell lung cancer with epidermal growth factor receptor mutations. *Br J Cancer* 2006;95:998–1004.
24. Sutani A, Nagai Y, Udagawa K, et al. Gefitinib for non-small-cell lung cancer patients with epidermal growth factor receptor gene mutations screened by peptide nucleic acid-locked nucleic acid PCR clamp. *Br J Cancer* 2006;95:1483–1489.
25. Ebi N, Semba H, Tokunaga SJ, et al. Lung Oncology Group in Kyushu, Japan. A phase II trial of gefitinib monotherapy in chemotherapy-naïve patients of 75 years or older with advanced non-small cell lung cancer. *J Thorac Oncol* 2008;3:1166–1171.
26. Jackman DM, Yeap BY, Lindeman NI, et al. Phase II clinical trial of chemotherapy-naive patients > or = 70 years of age treated with erlotinib for advanced non-small-cell lung cancer. *J Clin Oncol* 2007; 25:760–766.
27. Wheatley-Price P, Ding K, Seymour L, Clark GM, Shepherd FA. Erlotinib for advanced non-small-cell lung cancer in the elderly: an analysis of the National Cancer Institute of Canada Clinical Trials Group Study BR.21. *J Clin Oncol* 2008;26:2350–2357.
28. Chen YM, Tsai CM, Fan WC, et al. Phase II randomized trial of erlotinib or vinorelbine in chemonaive, advanced, non-small cell lung cancer patients aged 70 years or older. *J Thorac Oncol* 2012;7:412–418.
29. Inoue A, Saijo Y, Maemondo M, et al. Severe acute interstitial pneumonia and gefitinib. *Lancet* 2003;361:137–139.

Imaging, Diagnosis, Prognosis

Clinical Cancer Research

A Prospective PCR-Based Screening for the *EML4-ALK* Oncogene in Non–Small Cell Lung Cancer

Manabu Soda[1], Kazutoshi Isobe[2], Akira Inoue[6], Makoto Maemondo[7], Satoshi Oizumi[8], Yuka Fujita[9], Akihiko Gemma[3], Yoshihiro Yamashita[1], Toshihide Ueno[1], Kengo Takeuchi[4], Young Lim Choi[1,5], Hitoshi Miyazawa[10], Tomoaki Tanaka[10], Koichi Hagiwara[10], and Hiroyuki Mano[1,5,11], for the North-East Japan Study Group and the ALK Lung Cancer Study Group

Abstract

Purpose: *EML4-ALK* is a lung cancer oncogene, and ALK inhibitors show marked therapeutic efficacy for tumors harboring this fusion gene. It remains unsettled, however, how the fusion gene should be detected in specimens other than formalin-fixed, paraffin-embedded tissue. We here tested whether reverse transcription PCR (RT-PCR)-based detection of *EML4-ALK* is a sensitive and reliable approach.

Experimental Design: We developed a multiplex RT-PCR system to capture *ALK* fusion transcripts and applied this technique to our prospective, nationwide cohort of non–small cell lung cancer (NSCLC) in Japan.

Results: During February to December 2009, we collected 916 specimens from 853 patients, quality filtering of which yielded 808 specimens of primary NSCLC from 754 individuals. Screening for *EML4-ALK* and *KIF5B-ALK* with our RT-PCR system identified *EML4-ALK* transcripts in 36 samples (4.46%) from 32 individuals (4.24%). The RT-PCR products were detected in specimens including bronchial washing fluid ($n = 11$), tumor biopsy ($n = 8$), resected tumor ($n = 7$), pleural effusion ($n = 5$), sputum ($n = 4$), and metastatic lymph node ($n = 1$). The results of RT-PCR were concordant with those of sensitive immunohistochemistry with ALK antibodies.

Conclusions: Multiplex RT-PCR was confirmed to be a reliable technique for detection of *ALK* fusion transcripts. We propose that diagnostic tools for *EML4-ALK* should be selected in a manner dependent on the available specimen types. FISH and sensitive immunohistochemistry should be applied to formalin-fixed, paraffin-embedded tissue, but multiplex RT-PCR is appropriate for other specimen types. *Clin Cancer Res; 18(20); 5682–9. ©2012 AACR.*

Introduction

An oncogenic fusion between the echinoderm microtubule-associated protein–like 4 gene (*EML4*) and the anaplastic lymphoma kinase gene (*ALK*) was discovered by functional screening with a non–small cell lung cancer (NSCLC) specimen (1). *EML4* and *ALK* are located within a short distance (~12 Mbp) of each other on the short arm of human chromosome 2, and a small inversion involving the 2 loci is responsible for generation of the *EML4-ALK* fusion in lung cancer. The EML4-ALK tyrosine kinase undergoes constitutive dimerization through a coiled-coil domain within EML4, resulting in kinase activation and conferring potent transforming ability (2, 3). Transgenic mice expressing *EML4-ALK* in lung alveolar cells develop multiple adenocarcinoma nodules soon after birth, but treatment with an ALK inhibitor results in the rapid clearance of such nodules, confirming the addiction of EML4-ALK–positive tumors to the kinase activity of the fusion protein (4). The therapeutic efficacy of ALK inhibitors has been confirmed in other transgenic mice expressing EML4-ALK (5).

Several ALK inhibitors have already entered clinical trials or are under preclinical development (6–10). Marked therapeutic efficacy of one such compound, crizotinib, has been described in patients with NSCLCs positive for *EML4-ALK*, with an overall response rate of 57% (7), and crizotinib was recently approved as a therapeutic drug by the U.S. Food

Authors' Affiliations: [1]Division of Functional Genomics, Jichi Medical University, Tochigi; [2]Department of Respiratory Medicine, Toho University Omori Medical Center; [3]Nippon Medical School Hospital; [4]Pathology Project for Molecular Targets, The Cancer Institute; [5]Department of Medical Genomics, Graduate School of Medicine, University of Tokyo, Tokyo; [6]Tohoku University Hospital; [7]Miyagi Cancer Center, Miyagi; [8]First Department of Medicine, Hokkaido University School of Medicine; [9]Asahikawa Medical Center, Hokkaido; [10]Saitama Medical University Hospital; and [11]CREST, Japan Science and Technology Agency, Saitama, Japan

Note: Supplementary data for this article are available at Clinical Cancer Research Online (http://clincancerres.aacrjournals.org/).

The nucleotide sequence of the novel *EML4-ALK* variant cDNA from patient J-#189 has been deposited in the DDBJ/EMBL/GenBank databases under the accession number AB663645.

Corresponding Author: Hiroyuki Mano, Division of Functional Genomics, Jichi Medical University, 3311-1 Yakushiji, Shimotsukeshi, Tochigi 329-0498, Japan. Phone: 81-285-58-7449; Fax: 81-285-44-7322; E-mail: hmano@jichi.ac.jp

doi: 10.1158/1078-0432.CCR-11-2947

Translational Relevance

The recent approval of an ALK inhibitor by the U.S. Food and Drug Administration has rendered urgent the development of a diagnostic scheme for tumors harboring *ALK* fusion genes. Whereas FISH is effective for analysis of formalin-fixed, paraffin-embedded (FFPE) tissue, how to test other types of specimen remains unsettled. We conducted a prospective, nationwide screening for *EML4-ALK*- or *KIF5B-ALK*–positive lung carcinomas in Japan with the use of a newly developed multiplex reverse transcription (RT)-PCR system. Various subtypes of *EML4-ALK* cDNA were identified in 36 of 808 specimens with adequate RNA quality. The RT-PCR results were concordant with those of immunohistochemistry, and *EML4-ALK* PCR products were detected in independent specimens from the same individuals. As far as we are aware, our study represents the first prospective RT-PCR–based screening for *EML4-ALK*, and it shows that multiplex RT-PCR is reliable for detection of the fusion gene in non-FFPE specimens.

and Drug Administration within a remarkably short period after target discovery (3, 11).

The failure of crizotinib treatment in individuals without oncogenic *ALK* fusions (12) and an adverse effect of treatment with gefitinib on the prognosis of patients with NSCLCs who do not harbor mutations of the EGF receptor (*EGFR*) gene (13) both suggest that ALK inhibitors should be administered only to patients positive for oncogenic ALK proteins. FISH-based detection of *ALK* rearrangements has proved to be of diagnostic use in the trials with crizotinib (7). Furthermore, detection of ALK proteins by sensitive immunohistochemistry (IHC) has been described (14, 15), and one such immunohistochemical screening approach resulted in the identification of another oncogenic ALK fusion, KIF5B-ALK (14). However, a substantial proportion of patients attending clinics are diagnosed with lung cancer on the basis of pathologic analysis of bronchial lavage fluid, pleural effusion, or sputum. Given that these specimens are not always suitable for the preparation of formalin-fixed, paraffin-embedded (FFPE) tissue required for FISH or IHC, individuals who are diagnosed solely by analysis of such specimens cannot receive EML4-ALK tests. To allow the sensitive detection of *EML4-ALK* and *KIF5B-ALK* in such specimens, we have now developed a multiplex reverse transcription (RT)-PCR system that captures the 2 *ALK* fusions, and we have tested its reliability as a diagnostic tool in our large-scale prospective cohort.

Materials and Methods

Prospective collection of NSCLC specimens

During February to December of 2009, we collected a total of 916 lung cancer specimens from 853 independent patients through our multicenter, nationwide networks in Japan. All specimens but resected tumors were mixed with RLT buffer (Qiagen) immediately after sampling, a step that markedly inhibits RNA degradation for up to 3 days at room temperature (data not shown). Resected tumor samples were snap-frozen and stored at −80°C until extraction of RNA and DNA. Portions of the samples were sent to Jichi Medical University (Tochigi, Japan) for multiplex RT-PCR analysis of *EML4-ALK* and *KIF5B-ALK* fusions and to Saitama Medical University (Saitama, Japan) for peptide nucleic acid–locked nucleic acid (PNA-LNA) PCR clamp analysis of *EGFR* mutations (16). All specimens were confirmed by pathologic analysis to contain malignant cells. More than half of the specimens were collected through the North-East Japan Study Group network according to the NEJ004 protocol. The study was approved by the Institutional Review Board of each participating center, and written informed consent was obtained from each study subject. All statistical analysis was conducted with 2-sided tests, and a $P < 0.05$ was considered statistically significant.

Clinicopathologic features of EML4-ALK–positive NSCLC

The clinicopathologic features of patients with *EML4-ALK*–positive or -negative tumors in our cohort are summarized in Table 1 and Supplementary Table S1. Consistent with previous observations, *EML4-ALK*–positive patients were significantly younger than those without *EML4-ALK* ($P < 0.001$, Student' t test) and were enriched in never or light smokers ($P < 0.001$, Fisher exact test). Our data also indicated that *EML4-ALK*–positive tumors are more likely to occur in women than in men ($P < 0.001$, Fisher exact test). In the present cohort, *EML4-ALK* was detected only in lung adenocarcinoma ($P < 0.001$, Fisher exact test), for which the fusion-positive rate was 6.11%.

A total of 718 specimens were screened for *EGFR* mutations, with such mutations being detected in 171 cases (23.8%). Whereas most *EML4-ALK*–positive tumors did not harbor *EGFR* mutations ($P = 0.002$, Fisher exact test), we did detect one tumor doubly positive in this regard. *EML4-ALK* and *EGFR* mutations are largely mutually exclusive (17, 18), but, importantly, such exclusiveness may not be absolute (19). Given that the presence of *EML4-ALK* and *EGFR* mutations in our doubly positive patient was examined with cells isolated from bronchial washing fluid, which was the only available specimen for molecular analysis in this individual, we were not able to determine whether there was a genuinely double-positive tumor in the lung or there were multiple independent tumors each positive for *EML4-ALK* or mutated *EGFR*.

We also attempted to examine the mutation status of *KRAS* among our 32 cases positive for *EML4-ALK*. We were able to sequence *KRAS* cDNAs for 26 of these patients, none of whom showed *KRAS* alterations (data not shown), confirming the mutual exclusivity of *EML4-ALK* and *KRAS* mutations (17, 20, 21).

Quality assessment of samples

Complementary DNA prepared from the specimens was first subjected to RT-PCR analysis with primers (5′-

Table 1. Characteristics of subjects positive for *EML4-ALK* by the RT-PCR diagnostic system.

Identification number	Sex/ age, y	Pathologic classification	Specimen type	*EML4-ALK* variant	Smoking history (pack-years)	TNM classification	Clinical stage	iAEP	*EGFR* mutation	*KRAS* mutation
J-#1	M/27	Adenocarcinoma	Sputum (2 different time points)	E13;A20	0	cT4N3M1	4	+	–	–
J-#4	F/39	Adenocarcinoma	Metastatic lymph node	E20;A20	NA	cTxN3M1	4	+	–	–
J-#7	M/74	Adenocarcinoma	Bronchial washing fluid	E13;A20	50	cT4N3M1	4	ND	–	–
J-#12	F/56	Adenocarcinoma	Resected tumor	E13;A20	0	cT1N0M0	1A	+	–	ND
J-#53	M/48	Adenocarcinoma	Tumor biopsy/sputum	E13;A20	0	cT3N2M1	4	+	–	–
J-#88	F/37	Adenocarcinoma	Pleural effusion	E13;A20	0	cT4N3M1	4	ND	–	–
J-#127	F/49	Adenocarcinoma	Tumor biopsy	E6a/b;A20	0.9	cT1N2M1	4	+	–	–
J-#189	F/37	Adenocarcinoma	Resected tumor	E14::ins2; ins56A20	0	cT2N1M1	4	+	–	–
J-#210	F/37	Adenocarcinoma	Resected tumor	E13;A20	0	cT4N2M1	4	ND	–	–
J-#215	F/61	Adenocarcinoma	Sputum	E13;A20	82	cT4N2M1	4	ND	–	–
J-#330	M/72	Adenocarcinoma	Pleural effusion/resected tumor (2 different regions)	E13;A20	0	cT4N1M1	4	+	–	–
J-#350	F/53	Adenocarcinoma	Pleural effusion	E13;A20	0	cT4N2M0	3B	ND	–	–
J-#378	F/78	Adenocarcinoma	Resected tumor	E13;A20	0	cT1N0M0	1A	ND	–	–
J-#385	F/80	Adenocarcinoma	Pleural effusion	E6a/b;A20	0	cT4N3M1	4	ND	–	–
J-#391	F/55	Adenocarcinoma	Tumor biopsy	E13;A20	16.5	cT2N2M1	4	+	–	ND
J-#392	F/38	Adenocarcinoma	Tumor biopsy	E13;A20	34	cT4N2M0	3B	+	–	ND
J-#393	F/42	Adenocarcinoma	Tumor biopsy	E13;A20	0	cT4N3M1	4	–	–	ND
J-#409	F/35	Adenocarcinoma	Tumor biopsy	E13;A20	0	cT4N0M0	3B	+	–	–
J-#422	M/69	Adenocarcinoma	Tumor biopsy	E6a/b;A20	0	cT2N2M0	3A	ND	–	–
J-#450	F/30	Adenocarcinoma	Bronchial washing fluid	E6a/b;A20	0	cT4N2M1	4	+	–	–
J-#530	F/55	Adenocarcinoma	Bronchial washing fluid	E13;A20	0	cT1N1M1	4	+	+	ND
J-#646	F/36	Adenocarcinoma	Bronchial washing fluid	E6a/b;A20	0	cT2N3M0	3B	ND	–	–
J-#657	F/62	Adenocarcinoma	Bronchial washing fluid	E13;A20	15	cT4N2M0	3B	ND	–	–
J-#759	F/32	Adenocarcinoma	Resected tumor	E13;A20	12	cT1N0M0	1A	ND	–	–
J-#771	M/32	Adenocarcinoma	Tumor biopsy	E6a/b;A20	15	cT1N3M1	3B	ND	–	–
J-#817	M/33	Adenocarcinoma	Pleural effusion	E13;A20	0	cT2N1M1	4	ND	–	–
J-#848	M/57	Adenocarcinoma	Bronchial washing fluid	E18;E20	0	cT4N2M0	3B	ND	–	–
J-#887	F/32	Adenocarcinoma	Bronchial washing fluid	E6a/b;A20	0	cTxN3M1	4	ND	–	ND
J-#927	M/36	Adenocarcinoma	Bronchial washing fluid	E6a/b;A20	30	cT4N3M1	4	–	–	–
J-#928	F/71	Adenocarcinoma	Bronchial washing fluid	E6a/b;A20	0	cT4N3M1	4	ND	–	–
J-#996	M/52	Adenocarcinoma	Bronchial washing fluid	E6a/b;A20	0	cT3N3M0	3B	ND	–	–
J-#1001	F/32	Adenocarcinoma	Bronchial washing fluid	E13;A20	6.5	cT2N2M1	4	+	–	–

Abbreviations: F, female; M, male; NA, not available; ND, not determined.

CTGTGGAGGCTGAACTGGATC-3′ and 5′-TCATCAACAAGCTCCACGGTG-3′) specific for the human ribonuclease P (RNase P) gene (GenBank accession number NM_005837). Given that we previously showed that the abundance of RNase P mRNA is similar to that of *EML4-ALK* mRNA in NSCLCs (data not shown), we used the successful amplification of RT-PCR products for RNase P as a threshold for selection of specimens for further analysis. Exclusion of small cell lung cancer specimens and filtering on the basis of RNase P mRNA abundance resulted in the isolation of 808 specimens of primary NSCLCs obtained from 754 individuals.

As shown in Supplementary Fig. S1, bronchial washing fluid, including bronchoalveolar lavage fluid and washing fluid for the brush, needle, forceps, and other implements used in bronchoscopy, constituted 66.3% of the 808 eligible samples, with the remaining specimens including pleural effusion (12.8%); surgically resected tumor (7.05%); sputum (4.33%); tumor biopsy tissue including that obtained by transbronchial lung biopsy and transbronchial needle aspiration (3.71%); peripheral blood (3.71%); cardiac effusion, spinal fluid, or ascites (1.36%); and metastatic lesions of NSCLCs (0.74%).

Multiplex RT-PCR analysis of EML4-ALK and KIF5B-ALK

Each specimen (with the exception of resected tumors) was mixed with an equal volume of RLT buffer at the Institute at which it was harvested. The resulting mixture was sent to Jichi Medical University, where DNA and RNA were extracted with the use of an automated BioRobot EZ1 workstation (Qiagen). The isolated RNA was subjected to RT with a ReverTra Ace qPCR RT kit (Toyobo), and the resulting cDNA was subjected to PCR for 50 cycles of incubation at 94°C for 15 seconds, 60°C for 30 seconds, and 72°C for 1 minute with AmpliTAQ Gold DNA polymerase (Applied Biosystems) and with 2 μmol/L of each of the following

primers: F-1, 5′-GCTTTCCCCGCAAGATGGACGG-3′; F-2, 5′-TACCAGTGCTGTCTCAATTGCAGG-3′; F-3, 5′-GTGCAGTGTTTAGCATTCTTGGGG-3′; F-4, 5′-AGCTACATCACACACCTTGACTGG-3′; F-5, 5′-TCAAGCACATCTCAAGAGCAAGTG-3′; F-6, 5′-ATCCTGCGGAACACTATTCAGTGG-3′; F-7, 5′-GACAGTTGGAGGAATCTGTCGATG-3′; F-8, 5′-CAGCTGAGAGAGTGAAAGCTTTGG-3′; and R-1, 5′-TCTTGCCAGCAAAGCAGTAGTTGG-3′. All PCR products were subjected to Sanger sequencing to confirm the presence of *EML4-ALK* or *KIF5B-ALK* cDNA.

Results

Multiplex RT-PCR system

In addition to the original *EML4-ALK* fusion cDNA in which exon 13 of *EML4* is fused to exon 20 of *ALK* in an in-frame manner (designated the E13;A20 variant by analogy with karyotype nomenclature; see http://atlasgeneticsoncology.org/Tumors/inv2p21p23NSCCLungID5667.html), 14 different variants of *EML4-ALK* have been described (1, 14, 21–27). Seven exons of *EML4* are theoretically capable of in-frame fusion with exon 20 of *ALK* (Fig. 1A), and all but the E1;A20 variant would be expected to produce an oncogenic EML4-ALK protein, given that the coiled-coil domain encoded by exon 2 is required for constitutive dimerization of EML4-ALK. In addition, 6 different exons of *KIF5B* are theoretically capable of in-frame fusion with exon 20 of *ALK* (Fig. 1A).

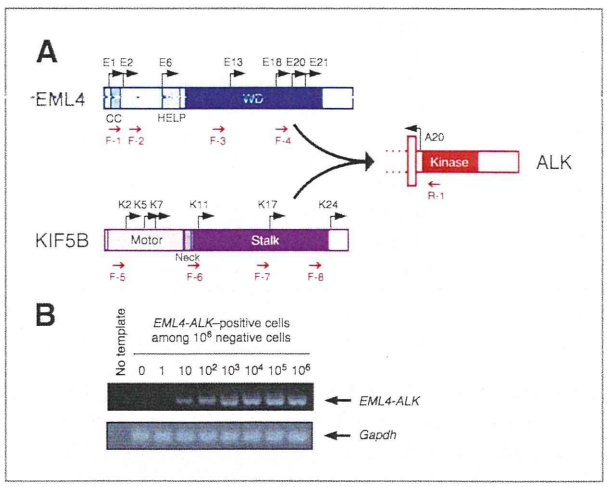

Figure 1. Multiplex RT-PCR system for detection of *EML4-ALK* and *KIF5B-ALK*. A, schematic representation of the structure of EML4, KIF5B, and ALK proteins. The positions of exons (E for *EML4* and K for *KIF5B*) theoretically capable of fusing in-frame to exon 20 (A20) of *ALK* are indicated by arrows. The positions of 8 forward primers (F-1 to F-8) and 1 reverse primer (R-1) for PCR are also indicated below the corresponding proteins. EML4 contains a coiled-coil domain (CC), a hydrophobic EMAP-like protein domain (HELP), and WD repeats (WD). KIF5B consists of an amino-terminal ATP-dependent motor domain, a neck region, and a stalk region. B, various numbers (0 to 1×10^6) of *EML4-ALK* (E13;A20)–positive BA/F3 cells (1) were mixed with a fixed number (1×10^6) of *EML4-ALK*–negative BA/F3 cells, and each mixture was analyzed with our multiplex RT-PCR system. A cDNA for mouse glyceraldehyde-3-phosphate dehydrogenase (*Gapdh*) was also amplified by PCR as an internal control with the primers 5′-TGTGTCCGTCGTGGATCTGA-3′ and 5′-CCTGCTTCACCACCTTCTTGA-3′.

To detect any such *EML4-ALK* or *KIF5B-ALK* fusion mRNAs, we developed a multiplex RT-PCR system. We had previously screened our archive of frozen tumors by RT-PCR analysis with 2 forward primers targeted to *EML4* and 1 reverse primer targeted to *ALK* (24), but such PCR conditions resulted in the amplification of products as large as ~1,300 bp for some variants. In this prospective study, we were faced with the analysis of a large number of samples with different levels of RNA quality. If the size of PCR products varied substantially among different *EML4-ALK* or *KIF5B-ALK* variants, some variants with large PCR products might not be amplified efficiently from specimens with low RNA quality. To be able to diagnose all possible fusions even with such samples, we therefore designed 4 forward primers for each of *EML4* and *KIF5B* so that the size variation among all possible RT-PCR products is minimal (Fig. 1A). This new multiplex system faithfully detected all known fusion variants from *EML4-ALK*–positive specimens in our previous archive of NSCLCs (data not shown).

To examine the sensitivity of our RT-PCR system, we mixed *EML4-ALK*–expressing BA/F3 cells (0 to 1×10^6) with *EML4-ALK*–negative cells (1×10^6) and then subjected them to RT-PCR analysis. A fusion cDNA was readily identified even with 10 positive cells (0.001%) among 1×10^6 negative cells (Fig. 1B), showing the high sensitivity of the RT-PCR system.

To confirm the potential of our RT-PCR–based system, we compared it with a sensitive immunohistochemical approach and with FISH for the diagnosis of our archive of surgically resected and freshly frozen tumors with high RNA quality. Fifteen NSCLC specimens that previously stained positive by our sensitive immunohistochemical approach, which is based on an intercalated antibody-enhanced polymer (iAEP) method (14), were analyzed by RT-PCR and FISH together with 96 iAEP-negative specimens in a blinded manner. RT-PCR analysis of all these specimens ($n = 111$) yielded a diagnosis identical to that obtained with the iAEP method ($P = 7.3 \times 10^{-19}$, Fisher exact test; data not shown). Analysis of the same sample set by a split FISH assay with Vysis probes (Abbott Laboratories) revealed that all of the iAEP-positive cases showed a rearranged *ALK* locus, whereas one iAEP-negative sample gave a discordant result (negative by iAEP and RT-PCR but positive by FISH; Supplementary Fig. S2). The reason for this discrepant result remains unclear, but the multiple signals obtained with the 3′-*ALK* probe in the FISH analysis are indicative of amplification of the *ALK* gene or its adjacent region. Despite this discrepancy, the RT-PCR and iAEP data were highly concordant with the FISH results ($P = 1.2 \times 10^{-17}$, Fisher exact test). Compared with the iAEP method, therefore, both the sensitivity and specificity of our RT-PCR system were 100%. In comparison with the Vysis FISH, the sensitivity and specificity of RT-PCR were 93.8% and 100%, respectively.

Detection of EML4-ALK

Screening of the 808 eligible specimens with our multiplex RT-PCR system identified positive products in 36 samples (4.46%) obtained from 32 different individuals

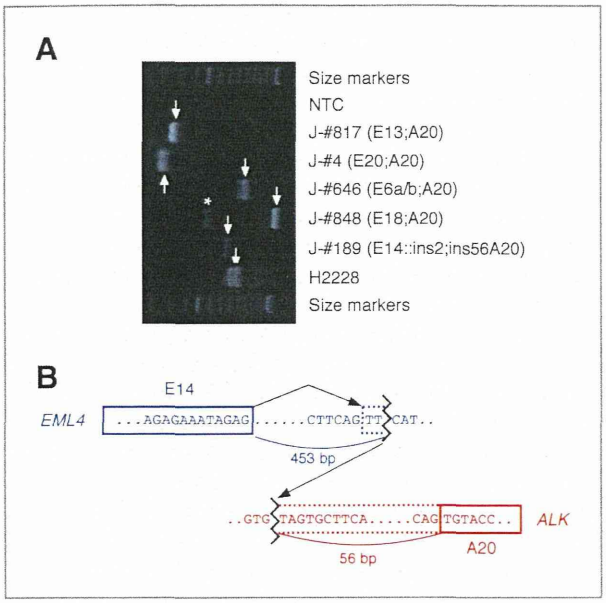

Figure 2. Multiplex RT-PCR detection of *EML4-ALK*–positive NSCLCs. A, RT-PCR products for each of the *EML4-ALK* variants identified in our cohort were separated by agarose gel electrophoresis. RT-PCR products spanning the *EML4-ALK* fusion points are indicated by arrows; the asterisk indicates a nonspecific product. An NSCLC cell line, H2228, harboring the E6a/b;A20 variant of *EML4-ALK* was used as a positive control for the PCR reaction. Size markers include a 50-bp DNA ladder (Invitrogen). NTC, no-template control. B, genomic structure of the fusion point for a novel variant of *EML4-ALK*. Nucleotide sequencing of the genomic PCR and RT-PCR products from patient J-#189 revealed that exon 14 of *EML4* (blue) was spliced to a TT sequence adjacent to the genomic ligation point, with transcription continuing in an in-frame manner into intron 19 and exon 20 of *ALK* (red).

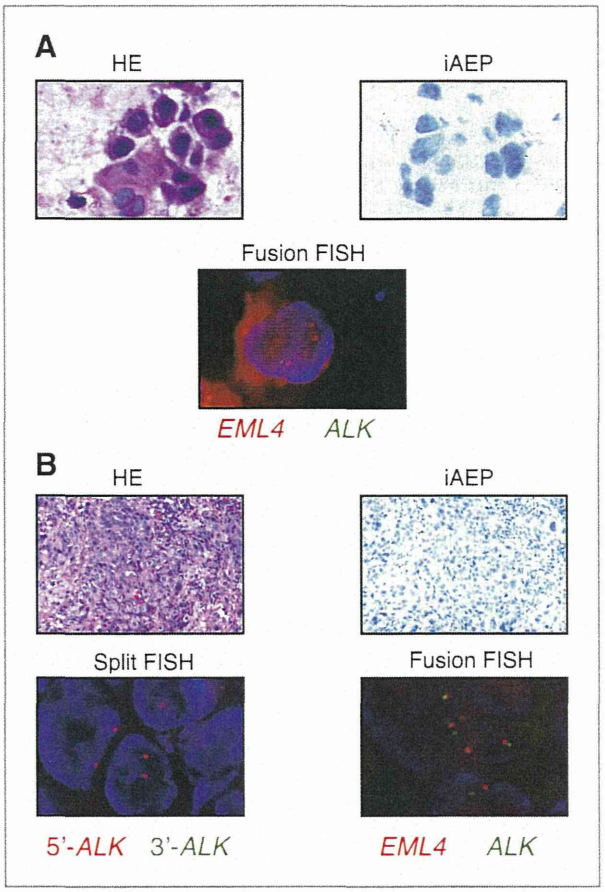

Figure 3. Specimens positive for *EML4-ALK* by RT-PCR but negative by iAEP-based IHC and by FISH. Sections of tumor biopsy specimens for J-#393 tumor (A) and J-#927 (B) were stained with hematoxylin-eosin (HE), subjected to immunohistochemical analysis by the iAEP method, and examined by split or fusion FISH. The color of fluorescence for the probes in each hybridization is indicated below the FISH images. Nuclei are stained blue with 4′,6-diamidino-2-phenylindole (DAPI).

(4.24%; Table 1, Fig. 2A). Nucleotide sequencing of each PCR product identified 19 cases positive for the E13;A20 variant, 10 cases for E6a/b;A20, a single case each for E18;A20, E20;A20, and a novel variant. *EML4-ALK* was detected in a wide range of specimens including bronchial washing fluid ($n = 11$), tumor biopsy ($n = 8$), resected tumor ($n = 7$), pleural effusion ($n = 5$), sputum ($n = 4$), and metastatic lymph node ($n = 1$). We did not detect any *KIF5B-ALK* cDNAs, confirming the rarity of this fusion gene.

Importantly, an E13;A20 product was consistently identified in both of the sputa obtained at different time points from patient J-#1. Likewise, an E13;A20 product was detected in both the tumor biopsy and sputum from patient J-#53 as well as in the pleural effusion and 2 resected tumor specimens from patient J-#330, supporting the reliability of our RT-PCR approach.

Sequence determination for the RT-PCR product from patient J-#189 revealed that exon 14 of *EML4* was fused to exon 20 of *ALK* with an intervening sequence. Genomic PCR analysis of the J-#189 specimen with a forward primer targeted to exon 14 of *EML4* and a reverse primer targeted to exon 20 of *ALK* yielded a specific product, nucleotide sequencing of which revealed that a position 453 bp downstream of *EML4* exon 14 was ligated to a position 56 bp upstream of *ALK* exon 20 (Fig. 2B). In the transcript of this fusion gene, exon 14 of *EML4* is thus spliced to a TT sequence that is located within *EML4* intron 14 and which is directly ligated to intron 19 of *ALK*. This splicing event results in an in-frame fusion between the mRNA sequences derived from *EML4* and *ALK*. Furthermore, a full-length cDNA for this variant, here designated E14::ins2;ins56A20, was isolated by RT-PCR analysis (Supplementary Fig. S3), and the potent transforming ability of the encoded protein was confirmed with an *in vitro* focus formation assay (Supplementary Fig. S4).

Comparison between multiplex RT-PCR and sensitive IHC

Finally, we applied the iAEP method to the *EML4-ALK*–positive cases for which FFPE specimens were also available ($n = 15$). All but 2 cases (J-#393 and J-#927) manifested clear immunoreactivity with antibodies to ALK (Table 1). FISH analysis of these 2 specimens also failed to detect the *EML4-ALK* rearrangements (Fig. 3). Given that genomic DNA was not available for the tumor of patient J-#393, we

were not able to determine whether the PCR result was a false-positive. For J-#927, however, PCR analysis of genomic DNA with a forward primer targeted to *EML4* exon 6 and a reverse primer to *ALK* exon 20 resulted in the amplification of an approximately 8.8-kbp genomic fragment, nucleotide sequencing of which revealed a fusion event between intron 6 of *EML4* and intron 19 of *ALK* (Supplementary Fig. S5). Isolation of the genomic fusion point thus indicates that J-#927 indeed harbors an *EML4-ALK*–positive tumor.

Discussion

We have conducted a large-scale, prospective screening for *EML4-ALK* with an RT-PCR–based approach. Whereas RNA extraction and cDNA synthesis add extra labor to the diagnostic procedure, certain introns of *EML4* are too large (intron 6 spans >16 kbp, for instance) for reliable amplification by genomic PCR. We therefore adopted RT-PCR as the method for our prospective screening. Specific PCR products were successfully isolated from different types of specimen, even from sputum (J-#1, J-#53, J-#215) and washing fluid of a tumor biopsy needle (J-#530). Multiple positive results obtained with different specimens of the same individuals further reinforce the reliability of our multiplex RT-PCR system as a diagnostic tool for *EML4-ALK*–positive tumors. Importantly, a subset of *EML4-ALK*–positive individuals diagnosed in the present study entered a clinical trial for crizotinib, and the response rate of the evaluable patients ($n = 9$) was 100% with this drug, again verifying the accuracy of our RT-PCR–based diagnosis.

The frequency of *EML4-ALK* in our cohort was 4.24% for all NSCLC cases and 6.11% for lung adenocarcinoma, values similar to those obtained in previous studies (20, 21). However, our prevalence data might be overestimates because the knowledge of mutual exclusiveness for *EML4-ALK* and *EGFR* mutations may have affected patient selection for our specimen collection. Indeed, *EGFR* mutation frequency among our cohort (23.8%) is slightly lower than that (30.9%) determined in a previous large-scale screening in Japan (28).

The clinicopathologic features of patients with *EML4-ALK*–positive tumors determined in the present study are also in agreement with those previously described, with a bias toward a young age, adenocarcinoma histology, and never or light smoking. Whereas a previous large-scale screening for *EML4-ALK* based on FISH did not detect a sex preference for the fusion gene (7), our cohort revealed a significant female preference. Such a sex difference was evident even among individuals below 40 years of age ($P = 0.03$, Fisher' exact test) and among those with an adenocarcinoma histology ($P = 0.005$, Fisher' exact test). Further large-scale studies are warranted to determine whether this uneven sex distribution of *EML4-ALK* is related to particular clinicopathologic features or ethnic groups.

Given that *EML4-ALK* and *EGFR* mutations are almost mutually exclusive and that the fusion gene is enriched in lung adenocarcinoma with an early onset, it should prove to be clinically beneficial to pay special attention to such subsets of patients. Indeed, *EML4-ALK* was detected in 27.7% of *EGFR* mutation–negative adenocarcinomas in individuals of younger than 50 years and in 50.0% of those in individuals of younger than 40 years in our cohort. Given the marked efficacy of ALK inhibitors in patients with *EML4-ALK*–positive NSCLCs (7), however, physicians should not dismiss the diagnosis in other subsets of patients. For example, *EML4-ALK* was even detected in an 80-year-old woman and in another woman with an intense smoking history (82 pack-years; Table 1).

Multiplex RT-PCR has both advantages and disadvantages compared with other techniques. Importantly, the accuracy of RT-PCR–based diagnosis depends markedly on the RNA quality of specimens. In our cohort, for instance, 71 (7.75%) of the initial 916 specimens were excluded from *EML4-ALK* screening because of a failure to obtain PCR products for RNase P (the other 37 samples were excluded because they were not NSCLCs). Low RNA quality thus clearly hampers reliable RT-PCR–based diagnosis.

Also, as expected, there was a large variation in the PCR cycle number required for successful amplification among specimens. In our cohort, 50 cycles of PCR allowed detection of PCR products for all positive cases, but such extensive amplification may also generate nonspecific products (as shown in Fig. 2A). Further optimization of primer sequences or combinations may minimize the generation of such byproducts. Furthermore, whereas our system should be able to capture all in-frame fusions of *ALK* to *EML4* or *KIF5B*, it is not capable in its present form of detecting *ALK* fusions to other partners, such as *KLC1-ALK*, which was recently shown to be present infrequently in NSCLCs (29).

On the other hand, RT-PCR can be readily applied to specimens such as sputum, bronchial washing fluid, or pleural effusion that may not be suitable for preparation of FFPE samples. Whereas the latter 2 specimen types can be used for the preparation of cell blocks suitable for analysis by FISH or IHC, this procedure may not be as widely adopted in the clinic as is FISH or IHC. More importantly, it is difficult to generate cell blocks or FFPE samples from sputum. Our current prospective screening identified 4 *EML4-ALK*–positive sputa of 35 samples (Table 1, Supplementary Fig. S1), showing that sputum is a suitable specimen for RT-PCR analysis. Indeed, sputum was the only available specimen from patient J-#215 both for the diagnosis of NSCLCs and for the detection of *EML4-ALK*. If RT-PCR had not been applied to this patient's sputum, we would not have been able to identify her tumor as positive for *EML4-ALK*, and she would not have had the chance to receive treatment with an ALK inhibitor in Japan.

Furthermore, PCR-based detection of *EML4-ALK* should have a higher analytic sensitivity compared with IHC or FISH (Fig. 1B). Even with sputum obtained from a patient with chronic bronchitis, RT-PCR was able to readily detect *EML4-ALK* at a concentration of 10 positive cells/mL (1). Thus, provided that RNA is not substantially degraded, RT-PCR–based diagnosis is expected to have a strong advantage

with regard to the detection of low numbers of *EML4-ALK*–positive cells.

Ideally, every NSCLC case should be examined for the presence of *EML4-ALK*, with a sensitive and accurate diagnostic strategy for the oncogenic fusion being essential for the adoption of ALK inhibitors in the clinic. Given the reliable detection of *EML4-ALK* mRNA by multiplex RT-PCR shown in the present study, we propose the following scheme for the comprehensive diagnosis of *EML4-ALK*–positive NSCLCs. For sputum, bronchial lavage fluid, pleural effusion, or other specimens that may not be suitable for the preparation of FFPE tissue, multiplex RT-PCR should be applied to detect *ALK* fusion mRNAs. In contrast, given that FFPE specimens usually have fragmented RNA, they should be subjected to FISH and to sensitive immunohistochemical analysis such as that described previously (14, 15). Furthermore, FISH or IHC can be applied to cell blocks prepared from some non-FFPE specimens. No single technique is therefore able to detect *EML4-ALK* in all types of specimen, and appropriate tests should be chosen on the basis of the specimens available for a given patient.

Disclosure of Potential Conflicts of Interest

H. Mano is the CEO of CureGene Co., Ltd.; has commercial research grant from Illumina, Inc. and Astellas Pharma Inc.; has ownership interest (including patents); and is on the consultant/advisory board of Chugai Pharmaceutical, Astellas Pharma Inc., and Daiichi Sankyo Co., Ltd. No potential conflicts of interest were disclosed by the other authors.

Authors' Contributions

Conception and design: K. Hagiwara, H. Mano
Development of methodology: K. Takeuchi, Y.L. Choi
Acquisition of data (provided animals, acquired and managed patients, provided facilities, etc.): M. Soda, K. Isobe, A. Inoue, S. Oizumi, Y. Fujita, A. Gemma, Y. Yamashita, K. Takeuchi, H. Miyazawa, T. Tanaka, K. Hagiwara
Analysis and interpretation of data (e.g., statistical analysis, biostatistics, computational analysis): M. Soda, T. Ueno, H. Mano
Writing, review, and/or revision of the manuscript: S. Oizumi, A. Gemma, K. Hagiwara, H. Mano
Administrative, technical, or material support (i.e., reporting or organizing data, constructing databases): M. Maemondo, K. Takeuchi, K. Hagiwara
Study supervision: H. Mano

Grant Support

This study was supported in part by a grant for Research on Human Genome Tailor-made from the Ministry of Health, Labor, and Welfare of Japan; by Grants-in-Aid for Scientific Research from the Ministry of Education, Culture, Sports, Science, and Technology of Japan; and by grants from the Japan Society for the Promotion of Science, from Takeda Science Foundation, from Mochida Memorial Foundation for Medical and Pharmaceutical Research, from The Mitsubishi Foundation, and from The Sagawa Foundation for Promotion of Cancer Research.

The costs of publication of this article were defrayed in part by the payment of page charges. This article must therefore be hereby marked *advertisement* in accordance with 18 U.S.C. Section 1734 solely to indicate this fact.

Received November 17, 2011; revised June 26, 2012; accepted August 3, 2012; published OnlineFirst August 20, 2012.

References

1. Soda M, Choi YL, Enomoto M, Takada S, Yamashita Y, Ishikawa S, et al. Identification of the transforming *EML4-ALK* fusion gene in non-small-cell lung cancer. Nature 2007;448:561–6.
2. Mano H. ALKoma: a cancer subtype with a shared target. Cancer Discov 2012;2:495–502.
3. Shaw AT, Solomon B. Targeting anaplastic lymphoma kinase in lung cancer. Clin Cancer Res 2011;17:2081–6.
4. Soda M, Takada S, Takeuchi K, Choi YL, Enomoto M, Ueno T, et al. A mouse model for *EML4-ALK*-positive lung cancer. Proc Natl Acad Sci U S A 2008;105:19893–7.
5. Chen Z, Sasaki T, Tan X, Carretero J, Shimamura T, Li D, et al. Inhibition of ALK, PI3K/MEK, and HSP90 in murine lung adenocarcinoma induced by EML4-ALK fusion oncogene. Cancer Res 2010;70:9827–36.
6. Marzec M, Kasprzycka M, Ptasznik A, Wlodarski P, Zhang Q, Odum N, et al. Inhibition of ALK enzymatic activity in T-cell lymphoma cells induces apoptosis and suppresses proliferation and STAT3 phosphorylation independently of Jak3. Lab Invest 2005;85:1544–54.
7. Kwak EL, Bang YJ, Camidge DR, Shaw AT, Solomon B, Maki RG, et al. Anaplastic lymphoma kinase inhibition in non-small-cell lung cancer. N Engl J Med 2010;363:1693–703.
8. Katayama R, Khan TM, Benes C, Lifshits E, Ebi H, Rivera VM, et al. Therapeutic strategies to overcome crizotinib resistance in non-small cell lung cancers harboring the fusion oncogene EML4-ALK. Proc Natl Acad Sci U S A 2011;108:7535–40.
9. Lovly CM, Heuckmann JM, de Stanchina E, Chen H, Thomas RK, Liang C, et al. Insights into ALK-driven cancers revealed through development of novel ALK tyrosine kinase inhibitors. Cancer Res 2011;71:4920–31.
10. Sakamoto H, Tsukaguchi T, Hiroshima S, Kodama T, Kobayashi T, Fukami TA, et al. CH5424802, a selective ALK inhibitor capable of blocking the resistant gatekeeper mutant. Cancer Cell 2011;19:679–90.
11. Gerber DE, Minna JD. ALK inhibition for non-small cell lung cancer: from discovery to therapy in record time. Cancer Cell 2010;18:548–51.
12. Butrynski JE, D'Adamo DR, Hornick JL, Dal Cin P, Antonescu CR, Jhanwar SC, et al. Crizotinib in ALK-rearranged inflammatory myofibroblastic tumor. N Engl J Med 2010;363:1727–33.
13. Mok TS, Wu YL, Thongprasert S, Yang CH, Chu DT, Saijo N, et al. Gefitinib or carboplatin-paclitaxel in pulmonary adenocarcinoma. N Engl J Med 2009;361:947–57.
14. Takeuchi K, Choi YL, Togashi Y, Soda M, Hatano S, Inamura K, et al. KIF5B-ALK, a novel fusion oncokinase identified by an immunohistochemistry-based diagnostic system for ALK-positive lung cancer. Clin Cancer Res 2009;15:3143–9.
15. Mino-Kenudson M, Chirieac LR, Law K, Hornick JL, Lindeman N, Mark EJ, et al. A novel, highly sensitive antibody allows for the routine detection of ALK-rearranged lung adenocarcinomas by standard immunohistochemistry. Clin Cancer Res 2010;16:1561–71.
16. Nagai Y, Miyazawa H, Huqun, Tanaka T, Udagawa K, Kato M, et al. Genetic heterogeneity of the epidermal growth factor receptor in non-small cell lung cancer cell lines revealed by a rapid and sensitive detection system, the peptide nucleic acid-locked nucleic acid PCR clamp. Cancer Res 2005;65:7276–82.
17. Shaw AT, Yeap BY, Mino-Kenudson M, Digumarthy SR, Costa DB, Heist RS, et al. Clinical features and outcome of patients with non-small-cell lung cancer who harbor EML4-ALK. J Clin Oncol 2009;27:4247–53.
18. Horn L, Pao W. EML4-ALK: honing in on a new target in non-small-cell lung cancer. J Clin Oncol 2009;27:4232–5.
19. Tiseo M, Gelsomino F, Boggiani D, Bortesi B, Bartolotti M, Bozzetti C, et al. EGFR and EML4-ALK gene mutations in NSCLC: a case report of erlotinib-resistant patient with both concomitant mutations. Lung Cancer (Amsterdam, the Netherlands) 2011;71:241–3.
20. Inamura K, Takeuchi K, Togashi Y, Hatano S, Ninomiya H, Motoi N, et al. EML4-ALK lung cancers are characterized by rare other mutations, a TTF-1 cell lineage, an acinar histology, and young onset. Mod Pathol 2009;22:508–15.
21. Wong DW, Leung EL, So KK, Tam IY, Sihoe AD, Cheng LC, et al. The EML4-ALK fusion gene is involved in various histologic types of lung

cancers from nonsmokers with wild-type EGFR and KRAS. Cancer 2009;115:1723–33.
22. Choi YL, Takeuchi K, Soda M, Inamura K, Togashi Y, Hatano S, et al. Identification of novel isoforms of the *EML4-ALK* transforming gene in non-small cell lung cancer. Cancer Res 2008;68:4971–6.
23. Koivunen JP, Mermel C, Zejnullahu K, Murphy C, Lifshits E, Holmes AJ, et al. EML4-ALK fusion gene and efficacy of an ALK kinase inhibitor in lung cancer. Clin Cancer Res 2008;14:4275–83.
24. Takeuchi K, Choi YL, Soda M, Inamura K, Togashi Y, Hatano S, et al. Multiplex reverse transcription-PCR screening for *EML4-ALK* fusion transcripts. Clin Cancer Res 2008;14:6618–24.
25. Lin E, Li L, Guan Y, Soriano R, Rivers CS, Mohan S, et al. Exon array profiling detects EML4-ALK fusion in breast, colorectal, and non-small cell lung cancers. Mol Cancer Res 2009;7:1466–76.
26. Takahashi T, Sonobe M, Kobayashi M, Yoshizawa A, Menju T, Nakayama E, et al. Clinicopathologic features of non-small-cell lung cancer with EML4-ALK fusion gene. Ann Surg Oncol 2010;17:889–97.
27. Sanders HR, Li HR, Bruey JM, Scheerle JA, Meloni-Ehrig AM, Kelly JC, et al. Exon scanning by reverse transcriptase-polymerase chain reaction for detection of known and novel EML4-ALK fusion variants in non-small cell lung cancer. Cancer Genet 2011;204:45–52.
28. Toyooka S, Matsuo K, Shigematsu H, Kosaka T, Tokumo M, Yatabe Y, et al. The impact of sex and smoking status on the mutational spectrum of epidermal growth factor receptor gene in non small cell lung cancer. Clin Cancer Res 2007;13:5763–8.
29. Togashi Y, Soda M, Sakata S, Sugawara E, Hatano S, Asaka R, et al. KLC1-ALK: a novel fusion in lung cancer identified using a formalin-fixed paraffin-embedded tissue only. PLoS One 2012;7:e31323.

RESPIRATORY INVESTIGATION 50 (2012) 117–121

Contents lists available at SciVerse ScienceDirect

Respiratory Investigation

journal homepage: www.elsevier.com/locate/resinv

Case report

Miliary brain metastases in 2 cases with advanced non-small cell lung cancer harboring EGFR mutation during gefitinib treatment

Sayaka Mochizuki[a,*], *Naoki Nishimura*[a], *Akira Inoue*[b], *Koji Murakami*[b], *Toshihiro Nukiwa*[b], *Naohiko Chohnabayashi*[a]

[a]*Division of Pulmonary Medicine, St. Luke's International Hospital, 9-1Akashi-cho, Chuo-ku, Tokyo 104-8560, Japan*
[b]*Department of Respiratory Medicine, Tohoku University Hospital, Japan*

ARTICLE INFO

Article history:
Received 20 January 2012
Received in revised form
29 May 2012
Accepted 6 June 2012
Available online 15 July 2012

Keywords:
Miliary brain metastases
Lung adenocarcinoma
Epidermal growth factor receptor
Gefitinib
Whole brain radiotherapy

ABSTRACT

Here we report 2 cases of non-small cell lung cancer (NSCLC) with sensitive epidermal growth factor receptor (EGFR) gene mutation that developed miliary brain metastases characterized by dementia and disorientation during gefitinib therapy. One patient's therapy was switched from gefitinib to chemotherapy followed by whole brain radiotherapy (WBRT), which resulted in disease progression with coma. Gefitinib reinitiation improved the patient's symptoms. The other patient continued gefitinib during WBRT and achieved complete remission of the miliary metastases and lived 18 months longer. These results suggest that gefitinib concomitant with WBRT is an optional strategy for the treatment of patients with EGFR-mutated NSCLC with miliary metastases to prevent disease flare.

1. Introduction

As compared to standard chemotherapy, gefitinib, which is a tyrosine kinase inhibitor of epidermal growth factor receptor (EGFR-TKI), has demonstrated novel efficacy in patients with advanced non-small cell lung cancer (NSCLC) and a sensitive EGFR mutation [1]. Unfortunately, many patients who experience marked improvement following gefitinib therapy eventually face disease progression due to acquired resistance. The central nervous system (CNS) is a common site of relapse during EGFR-TKI treatment; however, the treatment strategy for such a situation remains unresolved [2]. The present study reports 2 characteristic cases of miliary brain metastasis under a gefitinib treatment regimen that were successfully managed using whole brain radiotherapy (WBRT) and concomitant gefitinib use.

1.1. *Case 1*

A 37-year-old Japanese woman visited our hospital presenting with weight loss and exertional dyspnea. Chest radiography showed bilateral diffuse granular opacity of the lungs and a mass in the right lower lung field (Fig. 1A). Transbronchial biopsy revealed lung adenocarcinoma (stage: cT4N3M1 [PUL, OSS], stage IV; Eastern Cooperative Oncology Group performance status: 4) with deletion of exon 19 of the EGFR gene. Gefitinib was administered as first-line treatment, resulting in almost complete response for 8 months. Despite the primary lesion and

*Corresponding author. Tel.: +81 3 3541 5151; fax: +81 3 3544 0649.
E-mail address: sayakam0920@gmail.com (S. Mochizuki).

2212-5345/$ - see front matter © 2012 The Japanese Respiratory Society. Published by Elsevier B.V. All rights reserved.
http://dx.doi.org/10.1016/j.resinv.2012.06.002

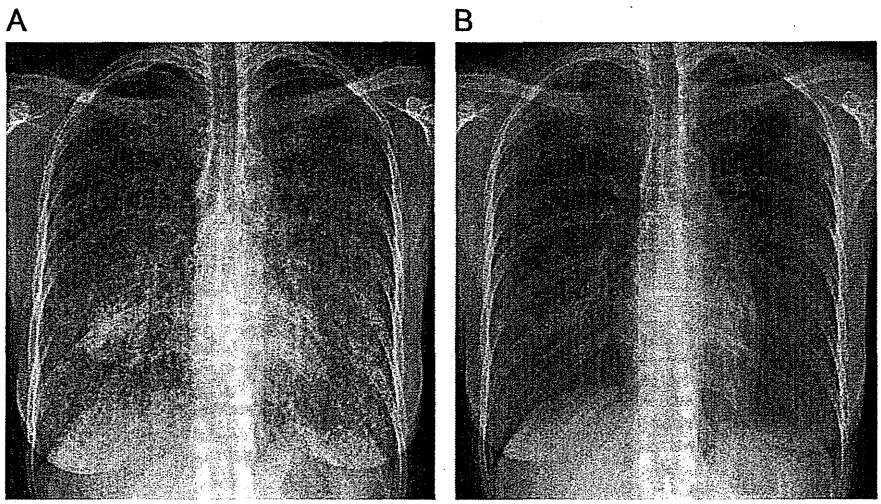

Fig. 1 – Case 1: Chest radiography. A: Bilateral diffuse granular opacity in the lungs and a mass in the right lower lung field. B: Marked improvement in primary lesion and miliary lung metastases, with disease progression to brain and bone metastases.

multiple lung metastases being well controlled (Fig. 1B), further metastases were observed in the brain and bones. Gefitinib therapy was then terminated and a second line chemotherapy with carboplatin and paclitaxel was initiated.

Seven days later, the patient complained of disorientation and difficulty in writing. Her dementia progressed to coma accompanied by mutism within several days of admission. Electroencephalography revealed generalized slowing in the delta and theta ranges. Laboratory results were unremarkable and her serum tested negative for the anti-Hu antibody. Findings of brain magnetic resonance imaging (MRI) with gadolinium-diethylenetriamine pentaacetic acid (Gd-DTPA) were unchanged from those of earlier examination (Fig. 2A). Lumbar puncture revealed atypical cells in the cerebrospinal fluid without the typical clinical features of meningitis carcinomatosa.

The patient was given WBRT (30 Gy/10 fractions) on day 16 after chemotherapy with carboplatin and paclitaxel to treat the brain metastases. Despite gradual improvement in consciousness with this treatment, 1 month after WBRT therapy, MRI scanning still showed enhanced miliary nodules in the brain (Fig. 2B); therefore, gefitinib was reinitiated via nasogastric tube on day 43 after chemotherapy. Her family hoped that the gefitinib therapy would improve her condition despite the treatment's possible side effects and ineffectiveness. One month later, the patient's condition improved dramatically and she was again able to speak and eat unaided; subsequent MRI revealed decreased brain metastases (Fig. 2C). She was discharged and spent 10 months at home under gefitinib treatment. The patient's memory disturbances gradually improved and she began to enjoy theatrical performances again. Her overall survival time after diagnosis was 1 year and 8 months.

1.2. *Case 2*

A 64-year-old Japanese woman with dry cough was referred to our hospital because of an abnormality detected on chest radiography by her family doctor. Subsequent chest computed tomography showed a mass in her right lower lung lobe with right pleural effusion and evidence of carcinomatous lymphangitis. Cytological examination of a transbronchial specimen demonstrated lung adenocarcinoma (stage: cT4N0M1 [PUL], stage IV; ECOG PS: 1), with deleted exon 19 of the EGFR gene. She was treated using gefitinib as first-line treatment, which led to a partial response lasting 7 months; however, both T2-weighted and Gd-DTPA-enhanced brain MRI performed as a periodic examination revealed numerous enhanced miliary metastases in the cerebral cortex and basal ganglia unaccompanied by clinical symptoms (Fig. 3A). Because no disease progression was observed in the other lesions, gefitinib therapy was continued and WBRT (36 Gy/12 fractions) was delivered concurrently. Subsequent brain MRI showed complete regression of the multiple brain metastases (Fig. 3B). Gefitinib treatment was maintained for 18 more months. The patient's overall survival time after diagnosis was 2 years and 5 months.

2. Discussion

Miliary brain metastasis, which is a rare form of CNS relapse, is characterized by perivascularly distributed diffuse miliary nodules unaccompanied by intraparenchymal invasion. Madow and Alpers first reported a case of carcinomatous encephalitis with these pathological features in 1951 [3]. The incidence of metastatic brain carcinomas was estimated at 3.8%, and lung adenocarcinoma was identified as the most common primary lesion [4,5]. Clinical symptoms included dementia and disorientation with rare progression to coma. Although establishing a diagnosis using imaging studies is sometimes difficult even in cases accompanied by dementia, MRI with Gd-DTPA is the most effective means of identifying miliary brain metastases [6]. Reports have described miliary brain metastases in some autopsy cases without imaging study abnormalities, indicating that antemortem diagnosis is difficult even after the onset of dementia. Our 2 cases here indicate that the treatment of miliary brain metastases

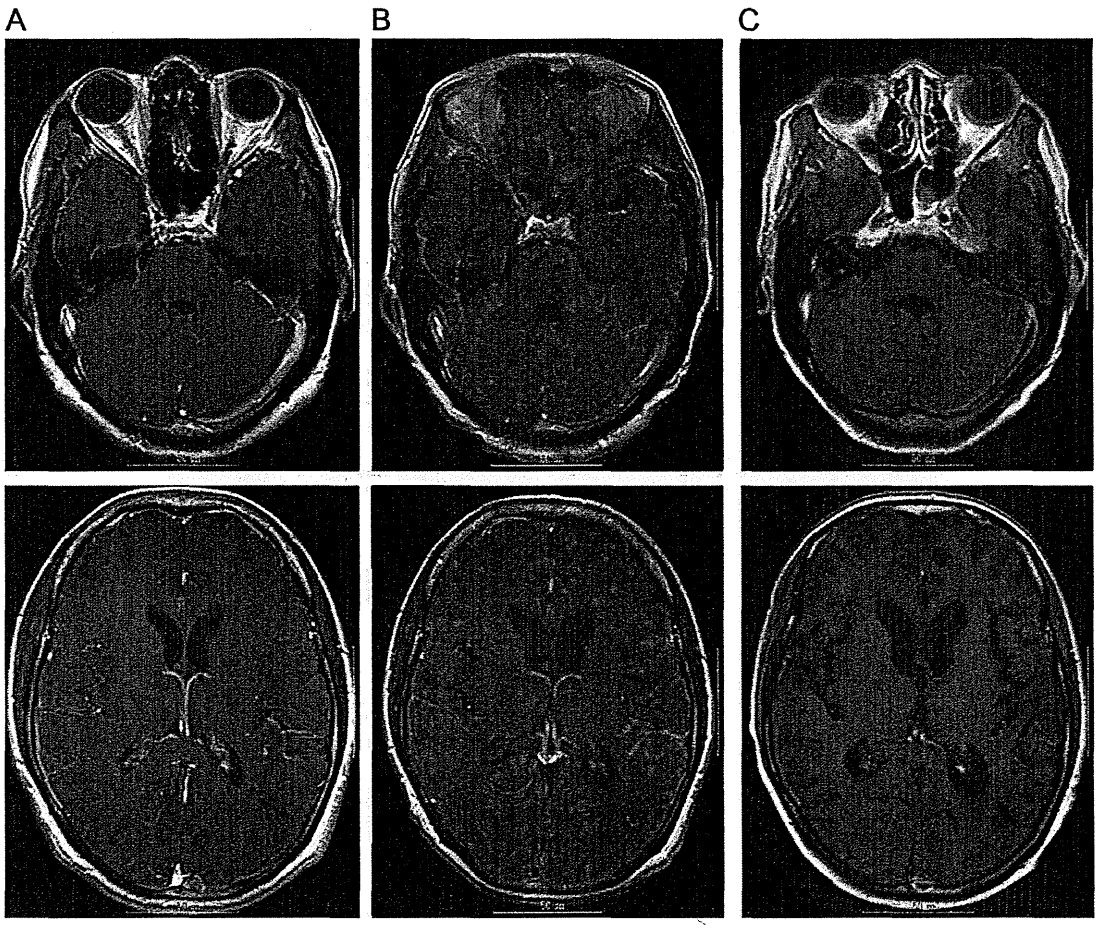

Fig. 2 – Case 1: Brain magnetic resonance imaging (MRI). A: With gadolinium-diethylenetriamine pentaacetic acid-enhanced MRI at 2 levels, the pons (upper) and basal ganglia (lower) showing no significant change after the patient became comatose. B: Multiple enhanced miliary nodules 1 month after radiation therapy. C: Decrease in brain metastatic lesions 2 months after radiation therapy.

without symptoms may be beneficial given this discrepancy between clinical symptoms and imaging findings.

Adenocarcinoma with a miliary pattern of lung metastases has recently been suggested as a distinct subtype that is primarily found in patients who have never smoked and is related to the exon 19 deletion *EGFR* mutation type [7]. Moreover, Sekine et al. reported a radiographic feature of miliary brain metastases in NSCLC with exon 19 deletion [8]. The 2 patients in the present study also showed adenocarcinoma with exon 19 deletion and miliary brain metastases. Because few reports have suggested an appropriate strategy for the management of such miliary brain metastases, further investigations are needed.

MRI scanning in both cases here showed the typical findings of miliary brain metastases suggested in earlier reports, but the 2 clinical courses were very different. In case 1, the patient demonstrated severe symptoms relating to a CNS disorder–dementia–that had progressed to coma with mutism. In contrast, in case 2, the patient was asymptomatic, and the brain metastases were detected by periodic MRI. Because the progression of CNS metastases quite often compromises a patient's quality of life, periodic MRI examinations may be beneficial for patients, although appropriate patient selection should be investigated further in terms of a cost–benefit balance. Regarding the treatment regimen, patients with miliary brain metastases arising from EGFR-mutated NSCLC might benefit from combined treatment with WBRT and gefitinib as illustrated in case 2, in which the patient's condition was maintained using the same strategy for over 18 months after the onset of miliary brain metastases.

Disease flare after discontinuation of EGFR-TKI has recently been a concern among patients with EGFR-mutated NSCLC [9]. The clinical course in case 1 was considered a typical pattern of disease flare after gefitinib discontinuation, and it successfully improved with readministration. With regard to toxicity, Ma et al. reported that the toxicities that were frequently observed during combined treatment using WBRT and gefitinib for NSCLC patients with brain metastasis included rash (86%), diarrhea (43%), nausea, vomiting, headache, and fatigue, most of which were mild and manageable [10]. Our patients also experienced rash, appetite loss, and

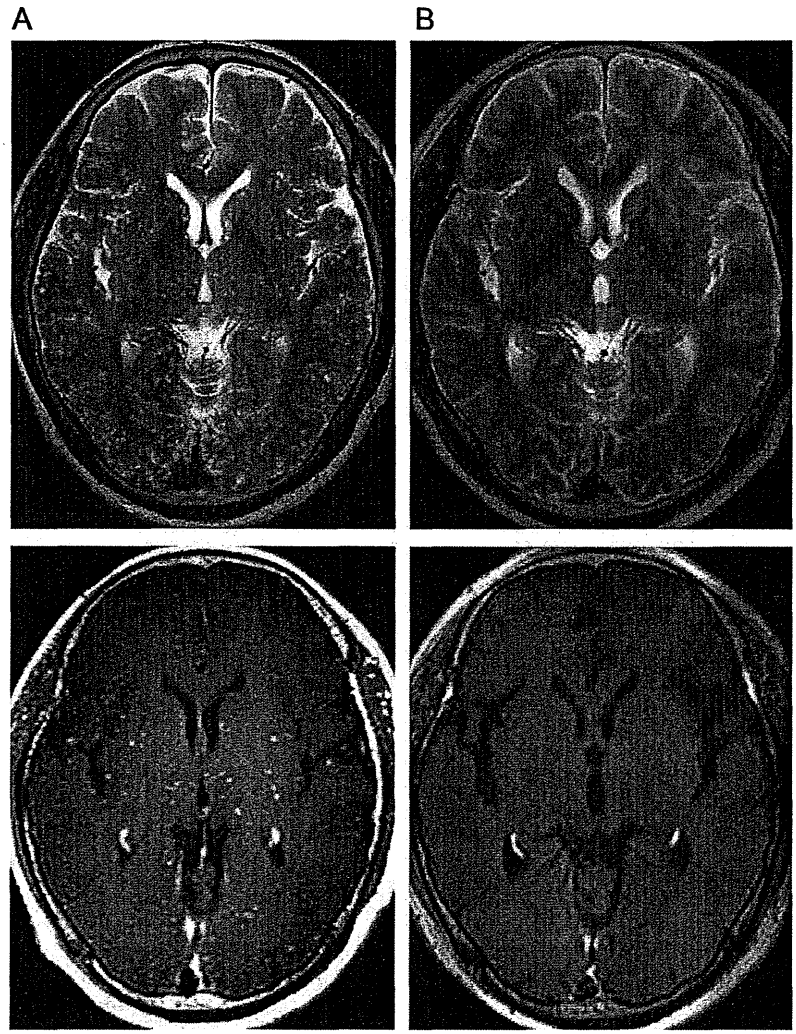

Fig. 3 – Case 2: Brain magnetic resonance imaging (MRI). A: Prior to radiotherapy, T2-weighted MRI scan (upper) showing multiple, small, high-intensity lesions in the cerebral cortex and basal ganglia. MRI enhanced with gadolinium-diethylenetriamine pentaacetic acid (Gd-DTPA) (lower) showing multiple miliary enhancing lesions at the same site. B: Nine months after radiation therapy, both T2-weighted (upper) and Gd-DTPA-enhanced MRI scans (lower) showed virtually complete disappearance of the metastatic lesions.

headache, although these toxicities were quite mild. In terms of efficacy and safety, this combination treatment merits further investigation.

Miliary brain metastases in EGFR-mutated NSCLC patients during treatment with EGFR-TKI must be considered a possibility. For a patient with such miliary brain metastases, combination treatment with WBRT and EGFR-TKI may be effective even in the presence of progressively disturbed consciousness.

Conflict of interest

Toshihiro Nukiwa received lecture fees from Boehringer Ingelheim.

Sayaka Mochizuki, Naoki Nishimura, Akira Inoue, Koji Murakami, Naohiko Chohnabayashi, they have no potential conflict of interest.

Sources of support

none

REFERENCES

[1] Maemondo M, Inoue A, Kobayashi K, et al. Gefitinib or chemotherapy for non-small-cell lung cancer with mutated EGFR. N Engl J Med 2010;362:2380–8.
[2] Ruppert AM, Beau-Faller M, Neuville A, et al. EGFR-TKI and lung adenocarcinoma with CNS relapse: interest of molecular follow-up. Eur Respir J 2009;33:436–40.
[3] Madow L, Alpers BJ. Encephalitic form of metastatic carcinoma. Arch Neurol Psychiatry 1951;65:161–73.
[4] Ogawa M, Kurahashi K, Ebina A, et al. Miliary brain metastasis presenting with dementia:progression pattern of cancer metastases in the cerebral cortex. Neuropathology 2007;27:390–5.

[5] Iguchi Y, Mano K, Goto Y, et al. Miliary brain metastases from adenocarcinoma of the lung: MR imaging findings with clinical and post-mortem histopathologic correlation. Neuroradiology 2007;49:35–9.
[6] Nakamura H, Toyama M, Uezu K, et al. Diagnostic dilemmas in oncology: case 1. Lung cancer with miliary brain metastases undetected by imaging studies. J Clin Oncol 2001;19:4340–1.
[7] Laack E, Simon R, Regier M, et al. Miliary never-smoking adenocarcinoma of the lung: strong association with epidermal growth factor receptor exon 19 deletion. J Thorac Oncol 2011;6:199–202.
[8] Sekine A, Kato T, Hagiwara E, et al. Metastatic brain tumors from non-small cell lung cancer with EGFR mutations: distinguishing influence of exon 19 deletion on radiographic feature. Lung Cancer 2012 (Epub ahead of print).
[9] Chaft JE, Oxnard GR, Sima CS, et al. Disease flare after tyrosine kinase inhibitor discontinuation in patients with EGFR-mutant lung cancer and acquired resistance to erlotinib or gefitinib: implications for clinical trial design. Clin Cancer Res 2011;17:6298–303.
[10] Ma S, Xu Y, Deng Q, et al. Treatment of brain metastasis from non-small cell lung cancer with whole brain radiotherapy and Gefitinib in a Chinese population. Lung Cancer 2009; 65:198–203.

Annals of Oncology

Annals of Oncology 23: 2914–2919, 2012
doi:10.1093/annonc/mds121
Published online 9 July 2012

An evaluation study of *EGFR* mutation tests utilized for non-small-cell lung cancer in the diagnostic setting

K. Goto[1*], M. Satouchi[2], G. Ishii[3], K. Nishio[4], K. Hagiwara[5], T. Mitsudomi[6], J. Whiteley[7], E. Donald[7], R. McCormack[7] & T. Todo[8]

[1]Division of Thoracic Oncology, National Cancer Center Hospital East, Chiba; [2]Department of Thoracic Oncology, Hyogo Cancer Center, Hyogo; [3]Pathology Division, Innovative Medical Research Center, National Cancer Center Hospital East, Chiba; [4]Department of Genome Biology, Kinki University School of Medicine, Osaka; [5]Department of Respiratory Medicine, Saitama Medical University, Saitama; [6]Department of Thoracic Surgery, Aichi Cancer Center Hospital, Aichi, Japan; [7]Department of Personalised Healthcare and Biomarkers, AstraZeneca Pharmaceuticals, Macclesfield, UK; [8]Department of Research and Development, AstraZeneca KK, Osaka, Japan

Received 19 December 2011; revised 2 March 2012; accepted 12 March 2012

Background: Epidermal growth factor receptor (*EGFR*) mutation is predictive for the efficacy of EGFR tyrosine kinase inhibitors in advanced non-small-cell lung cancer (NSCLC) treatment. We evaluated the performance, sensitivity, and concordance between five *EGFR* tests.

Materials and methods: DNA admixtures ($n = 34$; 1%–50% mutant plasmid DNA) and samples from NSCLC patients [116 formalin-fixed paraffin-embedded (FFPE) tissue, 29 matched bronchofiberscopic brushing (BB) cytology, and 20 additional pleural effusion (PE) cytology samples] were analyzed. *EGFR* mutation tests were PCR-Invader®, peptide nucleic acid-locked nucleic acid PCR clamp, direct sequencing, Cycleave™, and Scorpion Amplification Refractory Mutation System (ARMS)®. Analysis success, mutation status, and concordance rates were assessed.

Results: All tests except direct sequencing detected four mutation types at ≥1% mutant DNA. Analysis success rates were 91.4%–100% (FFPE) and 100% (BB and PE cytology), respectively. Inter-assay concordance rates of successfully analyzed samples were 94.3%–100% (FFPE; kappa coefficients: 0.88–1.00), 93.1%–100% (BB cytology; 0.86–1.00), and 85.0%–100% (PE cytology; 0.70–1.00), and 93.1%–96.6% (0.86–0.93) between BB cytology and matched FFPE.

Conclusions: All *EGFR* assays carried out comparably in the analysis of FFPE and cytology samples. Cytology-derived DNA is a viable alternative to FFPE samples for analyzing *EGFR* mutations.

Key words: cytology, EGFR mutation, FFPE, NSCLC, PCR

introduction

Epidermal growth factor receptor (*EGFR*) mutation is a key predictive factor for the efficacy of EGFR tyrosine kinase inhibitors in the treatment of patients with advanced non-small-cell lung cancer (NSCLC) [1–3]. *EGFR* mutation testing is necessary to enable the physician to offer the most suitable therapy for a patient with advanced NSCLC.

Four *EGFR* mutation tests, PCR-Invader® [4], peptide nucleic acid-locked nucleic acid (PNA-LNA) PCR clamp [5], PCR direct sequencing [6], and Cycleave PCR™ [7] are used commercially in Japan, with testing generally carried out by centralized contracted laboratories. The Scorpion Amplification Refractory Mutation System (ARMS)® [8] is another sensitive globally available method and in particular was used in the phase III Iressa Pan-Asia Study (IPASS) to determine *EGFR* mutation status [1, 9]. A variety of methods, including direct sequencing, PCR-Invader, PNA-LNA PCR clamp, fragment analysis, and Cycleave PCR, were used in the WJTOG3405 phase III study to select *EGFR* mutation-positive patients [2], and the PNA-LNA PCR clamp method was used in the NEJ002 study [3]. To date, a study to compare the sensitivity and concordance of methods for *EGFR* mutation testing in Japan has not been conducted.

Diagnostic practices, and therefore, samples available for *EGFR* mutation analysis, differ between laboratories and countries. Large surgical samples are optimal for *EGFR* mutation analysis but small tissue from a tumor biopsy is the most commonly used and preferred sample type for diagnosis by clinicians [10, 11]. In clinical practice, tissue samples are not always available for diagnosis, and cytology samples, including bronchofiberscopic brushing (BB) cytology and pleural effusion cytology samples, are used in Japan and increasingly globally.

The aim of this study was to evaluate the sensitivity and performance of different *EGFR* mutation tests using artificial DNA admixtures, and clinical samples including formalin-fixed

*Correspondence to: Dr K. Goto, Division of Thoracic Oncology, National Cancer Center Hospital East, Kashiwanoha, 6-5-1, Kashiwa, Chiba, 277-8577, Japan.
Tel: +81-4-7133-1111; Fax: +81-1-7131-4724; E-mail: kgoto@east.ncc.go.jp

paraffin-embedded (FFPE) tissue, BB cytology, and pleural effusion cytology samples from patients with NSCLC.

materials and methods

This was an observational study using control DNA admixtures and clinical samples. Patients provided written informed consent for samples to be used in research. The study was conducted as a collaborative research of AstraZeneca KK with National Cancer Center Hospital East (NCCHE) and Hyogo Cancer Center (HCC) after protocol approval by each Institutional Review Board and was conducted in accordance with ethical guidelines for epidemiological studies.

samples and DNA extraction

DNA admixtures

Four types of mutant plasmids were prepared including the *EGFR* mutation L858R, T790M, G719S, and E746-A750 deletion (nt del 2234-2249) in the Blue Heron pUC plasmid by Invitrogen Inc. (Tokyo, Japan). The sequence inserted into each plasmid corresponded with the longest sequence requirements spanning the exons across all of the methods to be evaluated, from −300 to +220 bp for exon 18 (for G719S) and from −200 to +200 bp for exons 19, 20, and 21 (for E746-A750 deletion, T790M, and L858R, respectively). Admixtures were prepared at Saitama Medical University Hospital. The plasmid preparations (5.4 ng/μl) were diluted with water and whole-human genomic DNA (12.5 ng/μl) (Promega Inc., Madison, WI) to prepare an admixture containing a 1 : 1 ratio (confirmed by Sanger sequencing) of copies of mutated and wild-type *EGFR* (5.4 fg/μl plasmid DNA, 10 ng/μl genomic DNA; referred to here as a 100% admixture). The 100% admixture solution was then diluted with genomic DNA to provide DNA solutions simulating those isolated from a clinical sample containing *EGFR*-mutated and wild-type cells at ratios of 50 : 50 (50% admixture), 25 : 75 (25%), 10 : 90 (10%), 5 : 95 (5%), 2 : 98 (2%), and 1 : 99 (1%). The samples were divided into aliquots for each laboratory, randomized and assigned an identification code, and 20 μl of each sample sent to the laboratories for mutation testing in a blinded manner. Ten wild-type control samples (from a single stock of genomic DNA) (10 ng/μl) were also distributed for testing.

formalin-fixed paraffin-embedded samples

In total, 120 FFPE NSCLC samples collected at NCCHE ($n = 100$) and HCC ($n = 20$) between December 2005 and October 2009 were used. Twelve consecutive sections (5-μm thickness), prepared by Sanritsu Co. Ltd (Tokyo, Japan) from each FFPE tissue block, were allocated as follows: sections 1 and 12, hematoxylin–eosin (H&E) staining; sections 2 and 7, PCR direct sequencing; sections 3 and 8, Cycleave PCR; sections 4 and 9, PCR-Invader; sections 5 and 10, PNA-LNA PCR clamp; sections 6 and 11, Scorpion ARMS. Samples were randomly assigned an identification code by Sanritsu Co. Ltd, with separate identification codes for the samples for PCR direct sequencing and Cycleave PCR (as they were to be analyzed by the same laboratory). A table of corresponding randomized identification codes was retained by AstraZeneca KK until analysis. H&E-stained sections (Sanritsu Co. Ltd) were reviewed by a single pathologist at NCCHE for histological type, tumor cell content, and tumor dimension in a blinded manner. DNA was extracted at each testing laboratory using their own standard operating procedures (SOPs), all of which utilized the QIAamp kit (QIAGEN Japan, Tokyo, Japan) (see supplemental Methods, available at *Annals of Oncology* online).

bronchofiberscopic brushing cytology samples

Thirty BB cytology samples (with matched FFPE samples available) obtained at NCCHE ($n = 10$) and HCC ($n = 20$) between 2006 and 2009 were used. Samples were collected by exfoliative cytodiagnosis brushing or curette washing in saline solution, without anticoagulant, and stored frozen. The BB cytology samples were randomized and assigned an identification code. The presence of tumor cells and histological type were confirmed by a pathologist at each center. DNA was extracted (QIAamp DNA Mini kit, QIAGEN Japan) at Kinki University of Medicine (Department of Genome Biology) and divided into 22 μl aliquots for analysis by the testing laboratories (direct sequencing was excluded due to the small amount of DNA anticipated, and for Scorpion ARMS, if the DNA concentration was <1 ng/μl, only exon 19 deletions, L858R, and T790M mutations were analyzed—see supplemental Methods, available at *Annals of Oncology* online).

pleural effusion cytology samples

Pleural effusion cytology samples were provided by NCCHE. Twenty pleural effusion cytology samples were collected from patients diagnosed with NSCLC (adenocarcinoma) between February 2009 and February 2010 and confirmed by a pathologist to contain tumor cells. Samples were frozen within 10 and 30 min of sampling and stored at −80°C. Frozen samples were thawed at 37°C and refrozen rapidly three times to disrupt the cells and ensure an even distribution and then divided into five equal aliquots that were sent to each of the testing laboratories. Samples were randomly assigned an identification code as for the FFPE samples. DNA was extracted at each laboratory using their own SOPs, all of which were based on the use of the QIAamp kit (see supplemental Methods, available at *Annals of Oncology* online).

EGFR mutation analysis

Samples were analyzed using five different *EGFR* mutation tests carried out by four different testing laboratories: PCR-Invader [4, 12] by BML Inc. (Tokyo, Japan); PNA-LNA PCR clamp [5] by Mitsubishi Chemical Medience Corp. (Tokyo, Japan); PCR direct sequencing (with the exception of the BB cytology samples, due to the anticipated tumor DNA yield based on published evidence regarding the detection limit of this method [13]) [6] by SRL Inc. (Tokyo, Japan), Cycleave PCR [7] also by SRL Inc., and Scorpion ARMS [14, 15] by Genzyme Analytical Services (Los Angeles, CA). Scorpion ARMS analysis employed the DxS *EGFR* Mutation Test Kit for research use only [QIAGEN Manchester (formerly DxS Ltd), UK] and was carried out according to the manufacturer's instructions with modifications described in the supplemental Methods (available at *Annals of Oncology* online). The other methods were carried out using each of the laboratories' experimental set up, with data analysis and quality control completed according to their own specific protocols (further details in the supplemental Methods, available at *Annals of Oncology* online). Samples were defined as mutation negative where sufficient material was present to generate a result but the presence of a mutation was not observed within the detection limit of the assay. The *EGFR* mutations detected by each *EGFR* mutation test are shown in supplemental Table S1 (available at *Annals of Oncology* online).

Analysis data (positive, negative, not detected, mutation type) and any supplemental information (e.g. failure of PCR amplification) were reported to AstraZeneca KK (Osaka, Japan).

statistical analysis

The correct determination rates (whether or not the positive/negative *EGFR* mutation assessment result was correct) and sensitivity (lowest percentage DNA admixture detected) by *EGFR* mutation type were assessed using DNA admixture samples for each *EGFR* mutation test.

The success and positive rates of each *EGFR* mutation test were determined using FFPE, and BB and pleural effusion cytology samples. The success rate was defined as the proportion of samples successfully analyzed

where it was possible to determine the mutation status. Samples were classified as unsuccessful where it was not possible to determine the mutation status, the PCR amplification failed, or if values of samples exceeded the cut-off value of Scorpion ARMS. The positive rate was defined as the number of samples analyzed as positive by each method as a proportion of the number of samples successfully analyzed. False-positive and false-negative rates were not determined, as no reference or 'gold standard' has been defined for *EGFR* mutation analysis.

The concordance rates and Cohen's kappa coefficients were determined between different methods of detection and between FFPE versus BB cytology sample types for mutation types commonly detectable by all assessed methods. Cohen's kappa coefficient was calculated as: kappa = (Po–Pe)/(1–Pe), where Po is the observed concordance rate and Pe is the expected probability of chance agreement.

results

patient samples

In total, 116 FFPE samples were evaluable for analysis, as four samples were confirmed not to contain NSCLC cells. The majority of samples were of adenocarcinoma histology and had a tumor cell content of at least 50%. Both tissue and tumor dimensions were ≤19 mm in most samples.

Of the 30 BB cytology samples (24 adenocarcinoma, four squamous, one adenosquamous, one large cell), one sample was excluded from the analysis because its matching FFPE sample was not judged as NSCLC. The samples were taken at a mean of 39 days (range 20–70 days) before operation and the mean DNA concentration was 8.73 ng/μl (range 0.2–40.3 ng/μl). All 20 pleural effusion cytology samples were assessable for analysis. Volumes of pleural effusion cytology samples used for each test method were 0.7–0.8 ml.

comparability of five *EGFR* mutation tests

DNA admixtures

PCR-Invader, PNA-LNA PCR clamp, Cycleave PCR, and Scorpion ARMS methods detected each of the *EGFR* mutation types L858R, T790M, G719S, and the in-frame deletion E746-A750 type I at ratios ranging from 1% to 50% of mutant/wild-type allele. PCR direct sequencing detected all types of mutations in samples containing 5%–50% of plasmid DNA but could not detect any of the mutations in the 1% mutant DNA admixture, nor exon 19 deletion or L858R in the 2% mutant DNA admixture. There were no false positives in wild-type samples.

formalin-fixed paraffin-embedded samples

Success rates of all five *EGFR* mutation tests were over 90% in FFPE samples (Table 1). Concordance rates between any two methods ranged from 85.3% to 99.1% including samples unsuccessfully analyzed and from 94.3% to 100% excluding samples unsuccessfully analyzed (supplemental Table S2, available at *Annals of Oncology* online). The rate of type 1 discordance (different mutations detected between the methods) was 3.4% (4/116 samples) and the rate of type 2 discordance (mismatch of mutation status between the methods) was 6.9% (8/116 samples) in FFPE samples (supplemental Table S3, available at *Annals of Oncology* online).

Unsuccessful rates of mutation analyses and discordance rates by tumor/sample characteristics for FFPE samples are shown in supplemental Figure S1 (available at *Annals of Oncology* online). Higher unsuccessful rates were associated with histological subtype [squamous cell carcinoma, 4/7 (57.1%)], older sample age [year of surgery 2006, 9/10 (90.0%)], and larger tumor dimension [20–29 mm, 3/15

Table 1. Success rate and *EGFR* mutation status determined by different *EGFR* mutation tests in FFPE, BB, and pleural effusion samples

Sample type and method	No. of samples successfully analyzed (%)	No. of mutation-positive samples (%)	No. of mutation-negative samples (%)
FFPE samples ($n = 116$)			
Scorpion ARMS	115 (99.1)	65 (56.5)	50 (43.5)
PCR-Invader	116 (100.0)	65 (56.0)	51 (44.0)
PNA-LNA PCR clamp	106 (91.4)	61 (57.5)	45 (42.5)
PCR direct sequencing	110 (94.8)	64 (58.2)	46 (41.8)
Cycleave PCR	116 (100.0)	63 (54.3)	53 (45.7)
BB cytology samples ($n = 29$)			
Scorpion ARMS	29 (100.0)	15 (51.7)	14 (48.3)
PCR-Invader	29 (100.0)	17 (58.6)	12 (41.4)
PNA-LNA PCR clamp	29 (100.0)	17 (58.6)	12 (41.4)
Cycleave PCR	29 (100.0)	16 (55.2)	13 (44.8)
Pleural effusion cytology samples ($n = 20$)			
Scorpion ARMS	20 (100.0)	11 (55.0)	9 (45.0)
PCR-Invader	20 (100.0)	11 (55.0)	9 (45.0)
PNA-LNA PCR clamp	20 (100.0)	10 (50.0)	10 (50.0)
PCR direct sequencing	20 (100.0)	11 (55.0)	9 (45.0)
Cycleave PCR	20 (100.0)	11 (55.0)	9 (45.0)

[a]Percentage calculated based on the number of samples successfully analyzed; *EGFR* mutation status was determined before the study and samples were selected to allow for an ~1:1 ratio of mutation-positive:mutation-negative samples.

ARMS, Amplification Refractory Mutation System; BB, bronchofiberscopic brushing; FFPE, formalin-fixed paraffin-embedded; PNA-LNA, peptide nucleic acid-locked nucleic acid.

(20.0%)] (supplemental Figure S1, available at *Annals of Oncology* online). Discordance rates tended to be higher in samples with low tumor cell content [0–20%, 2/10 (20.0%); 30–40%, 3/10 (30%)], smaller tumor dimension [0–9 mm, 11/53 (20.8%)], smaller tissue dimension [0–9 mm, 8/33 (24.2%)], and older sample age [year of surgery 2006, 2/10 (20.0%)] (supplemental Figure S1, available at *Annals of Oncology* online).

Concordance rates between five methods for the two major mutation types in FFPE samples were 81.8% (18/22) for exon 19 deletions and 87.2% (34/39) for L858R.

PCR direct sequencing identified rare mutations in six patients that were not detected by any other methods [V689L and E690V, E709V, V834L, I706T D770_N771 (insSVD), H773_V774(insPH)].

bronchofiberscopic brushing cytology samples

Success rates of the four *EGFR* mutation tests utilized for analysis of BB cytology samples were 100% (Table 1) and concordance rates between two methods ranged from 93.1% to 100% (supplemental Table S2, available at *Annals of Oncology* online). Discordances between two methods were found in two (6.9%) samples (supplemental Table S4, available at *Annals of Oncology* online). Both were type 2 discordances (mismatch of mutation status between the methods): in one sample, G719C detected by PCR-Invader and PNA-LNA PCR clamp was assessed as negative by Cycleave PCR (G719X not analyzed by Scorpion ARMS due to insufficient sample). In the remaining sample, L858R detected by PCR-Invader, PNA-LNA PCR clamp, and Cycleave PCR was assessed as negative by Scorpion ARMS.

Concordance rates between analysis of BB cytology and FFPE samples ranged from 65.5% to 96.6% including samples unsuccessfully analyzed and 93.1%–96.6% excluding samples unsuccessfully analyzed (supplemental Table S5, available at *Annals of Oncology* online). Discordances in analysis of BB cytology samples versus FFPE samples by the same detection method (excluding discordances due to unsuccessful mutation analysis of FFPE samples) were observed in three (10.3%) samples (supplemental Table S4, available at *Annals of Oncology* online); all were type 2 discordances (mismatch of mutation status between the methods).

pleural effusion cytology samples

Success rates of all five *EGFR* mutation tests were 100% (Table 1) and concordance rates between two methods ranged from 85.0% to 100% in the pleural effusion samples (supplemental Table S2, available at *Annals of Oncology* online). Discordances between five methods were found in three (15.0%) samples (supplemental Table S6, available at *Annals of Oncology* online). All were type 2 discordances (mismatch of mutation status between the methods): in one sample, an exon 19 deletion was detected by all methods except PCR direct sequencing; in another, an exon 19 deletion was only detected by Scorpion ARMS, Cycleave PCR, and PCR direct sequencing; and in the third sample, L858R was only detected by PCR-Invader. In one of the other 17 samples, PCR direct sequencing detected an additional mutation [exon 18 deletion (E709_T710>D)], which the other methods were not designed to assess.

discussion

Analysis of the control DNA admixture samples showed that the *EGFR* mutation tests had comparable sensitivity, with the exception of direct sequencing. The sensitivity of direct sequencing, although higher than expected and reported elsewhere [15], was lower than the other techniques.

The results of this study showed that all five *EGFR* mutation tests had comparable success rates (over 90%) in FFPE samples. These were consistently high success rates given that the fixation of some of the samples was not ideal (e.g. long fixation times). The success rates of direct sequencing were higher than anticipated based on previous studies of clinical samples. For example, in a recent study, ARMS and direct sequencing were used to detect known *EGFR* mutations in NSCLC FFPE samples, and ARMS was found to be a more sensitive and robust technique [13]. However, it should be recognized that even when utilizing the same technologies, differences in reagents, DNA quality, software, and crucially, primer design and amplicon size have a huge influence on direct sequencing success rates and mutation detection potential. Our results show that the processes implemented by the laboratory in this study are highly optimized for the detection of *EGFR* mutations from tumor DNA using direct sequencing. As the testing laboratories also carried out the DNA extraction (with the exception of BB cytology samples), the slight differences in DNA extraction and processes across the different laboratories could also impact on the overall performance of the test methods.

All the FFPE samples were examined by a pathologist and generally found to be of high quality and tumor content. The numbers of samples with different tumor/sample characteristics were too low to make any definitive conclusions regarding unsuccessful and discordance rates by these characteristics. However, sample unsuccessful rates appear to be associated with squamous cell carcinoma, older samples, and samples with long tumor dimension, all of which can make it difficult to extract DNA. In addition, discordance rates appeared higher in older samples or samples of low tumor cell content, short tumor dimension or short tissue dimension, where the quantities of DNA are small.

Concordance rates were generally over 85% (>94%, excluding samples unsuccessfully analyzed) between any two *EGFR* mutation tests in FFPE samples. The lowest concordance rates between the five methods were in comparison with the PNA-LNA PCR clamp method. As the PNA-LNA PCR clamp method also had a higher unsuccessful rate than the other methods, concordance rates were lower in comparison with other methods when including samples unsuccessfully analyzed. However, all kappa statistics were ≥ 0.70, indicating a high concordance of analysis results. Concordance rates for the two major *EGFR* mutation types, exon 19 deletions and L858R, across the five mutation tests in FFPE samples were also high (81.8% and 87.2%, respectively), illustrating the suitability of all